Unexpectedly high barriers to M–P rotation in tertiary phobane complexes : PhobPR behavior that is commensurate with tBu2PR

LISTER, Julia M., CARREIRA, Monica, HADDOW, Mairi F., HAMILTON, Alex, MCMULLIN, Claire L., ORPEN, A. Guy, PRINGLE, Paul G. and STENNETT, Tom E.

Published version

LISTER, Julia M., CARREIRA, Monica, HADDOW, Mairi F., HAMILTON, Alex, MCMULLIN, Claire L., ORPEN, A. Guy, PRINGLE, Paul G. and STENNETT, Tom E. (2014). Unexpectedly high barriers to M–P rotation in tertiary phobane complexes : PhobPR behavior that is commensurate with tBu2PR. Organometallics, 33 (3), 702-714.

Unexpectedly high barriers to M–P rotation in tertiary phobane complexes: PhobPR behavior that is commensurate with $^{t}Bu_2PR$

*Monica Carreira, Mairi F. Haddow, Alex Hamilton, Julia M. Lister, Claire L. McMullin, A. Guy Orpen, Paul G. Pringle**

School of Chemistry, University of Bristol, Cantock's Close, Bristol, BS8 1TS, UK.

* To whom correspondence should be addressed. E-mail: paul.pringle@bristol.ac.uk. Fax: +44 (0)117 929 0509. Tel: +44 (0)117 928 8114.

RECEIVED DATE

Graphic

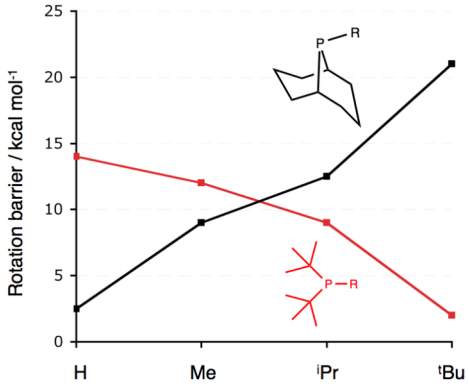

Abstract

The four isomers of 9-butylphosphabicyclo[3.3.1]nonane (*s*-PhobPBu, where Bu = *n*-, *sec*-, *iso*- and *tert*-butyl)) have been prepared. Seven isomers of 9-butylphosphabicyclo[4.2.1]nonane (a_5-PhobPBu, where Bu = *n*-, *iso*-, *sec*- and *tert*-butyl; a_7-PhobPBu, where Bu = *n*-, *iso*-, *sec*- and *tert*-butyl) have been identified in solution and some of the a_5 isomers have been isolated. The donor properties of the PhobPBu ligands have been compared in the light of the J_{PSe} values for PhobP(=Se)Bu isomers and ν_{CO} for the *trans*-[RhCl(CO)(PhobPBu)$_2$] complexes. The following complexes have been prepared: *trans*-[MCl_2(*s*-PhobPR)$_2$] M = Pt, R = ^{n}Bu (**1a**), ^{i}Bu (**1b**), ^{s}Bu (**1c**), ^{t}Bu (**1d**); *trans*-[MCl_2(a_5-PhobPR)$_2$] M = Pt, R = ^{n}Bu (**2a**), ^{i}Bu (**2b**); *trans*-[MCl_2(a_7-PhobPR)$_2$] M = Pt, R = ^{n}Bu (**3a**), ^{i}Bu (**3b**); *trans*-[MCl_2(*s*-PhobPR)$_2$] M = Pd, R = ^{n}Bu (**4a**), ^{i}Bu (**4b**); *trans*-[MCl_2(a_5-PhobPR)$_2$] M = Pd, R = ^{n}Bu (**5a**), ^{i}Bu (**5b**); *trans*-[MCl_2(a_7-PhobPR)$_2$] M = Pd, R = ^{n}Bu (**6a**), ^{i}Bu (**6b**). The crystal structures of **1-4a** and **1-6b** have been determined and of the 10 structures, 8 show an anti conformation with respect to the position of the ligand R groups and 2 show a syn conformation. Solution variable-temperature ^{31}P NMR studies reveal that all of the Pt and Pd complexes are fluxional on the NMR timescale. In each case, two species are present (assigned to be the syn and anti conformers) which interconvert with kinetic barriers in the range 9 to >19 kcal mol^{-1}. The greater the bulk of the R group of the PhobPR ligand, the higher the barrier. The magnitude of the rotation barriers for the PhobPR complexes are of the same order as those previously reported for ^{t}Bu$_2$PR complexes. Rotational profiles have been calculated for the model anionic complexes [PhobPR–$PdCl_3$]$^-$ using DFT and these faithfully reproduce the trends seen in the NMR studies of *trans*-[MCl_2(PhobPR)$_2$]. Rotational profiles have also been calculated for [^{t}Bu$_2$PR–$PdCl_3$]$^-$ and these show that the greater the bulk of the R group, the lower the rotational barrier, i.e. the opposite trend to [PhobPR–$PdCl_3$]$^-$. Calculated structures for the species at the maxima and minima in the curves indicate the origin of the restricted

rotation. In the case of the PhobPR complexes, it is the rigidity of the bicycle that enforces unfavorable H....Cl clashes involving the Pd–Cl groups with H atoms on the α- or β-carbon in the R substituent and H atoms in 1,3-axial sites within the phosphabicycle.

KEYWORDS. bicyclic phosphines, stereoelectronic effects, rotamers, fluxionality, platinum complexes, bulky phosphines

Introduction

The bicyclic tertiary phosphines known as phobanes (Chart 1)[1] were amongst the first tertiary phosphines to find application in industrial homogeneous catalysis: Shell's cobalt-catalysed reductive hydroformylation of long-chain alkenes is based on tertiary phobanes and has operated for over 40 years.[2] Subsequently, tertiary phobanes have found many other applications in homogeneous catalysis[3] and it is therefore of interest to explore the properties of their complexes[4] in the hope of providing insight into why phobanes are privileged ligands for certain types of catalysis.

Chart 1

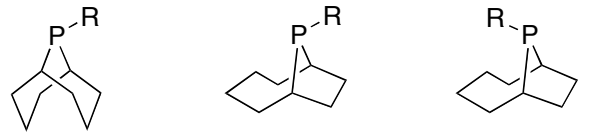

s-PhobPR a_5-PhobPR a_7-PhobPR

sym-phobane *asym*-phobane

Here we report *s*-, a_5- and a_7-PhobPBu (Bu = *n*-, *iso*-, *sec*- and *tert*-butyl) and show that the complexes *trans*-$[MCl_2(PhobPBu)_2]$ (M = Pt or Pd) are fluxional as a result of restricted M–P rotation. This observation runs counter to the prevailing maxim that there is essentially free rotation about M–P bonds unless the P-ligand contains very bulky substituents (e.g. $^tBu_2PR$) or the adjacent ligands are very bulky,[5,6,7] We report computational studies which suggest that it is the rigidity of the bicycle that is the source of the high barriers to M–P rotation in PhobPR complexes. The discovered high rigidity of PhobPR complexes may be significant in understanding the differences between the properties of complexes of phobanes and their acyclic analogues. It also shows that in one important respect, the coordination chemistry of the non-bulky PhobPR ligands resembles that of the omnipresent and very bulky $^tBu_2PR$ ligands.

Results and Discussion

Phobanes exist in the three diastereoisomeric forms shown in Chart 1 and we have previously reported[1] the diastereospecific synthesis of *s*-, a_5- and a_7-PhobP^{n}Bu. The isomeric butylphobanes in Chart 2 have now all been prepared, mostly as single diastereoisomers, by one of the routes shown in Scheme 1 (see Experimental for details). Others[8] have shown that *s*-PhobP^{i}Bu (as a mixture of diastereoisomers) can be prepared by hydrophosphination of 1,5-cyclooctadiene with ^{i}BuPH$_2$. All of the new phosphines were purified by distillation and characterized by a combination of ^{31}P, ^{13}C and ^{1}H NMR spectroscopy and high-resolution mass spectrometry.

Chart 2

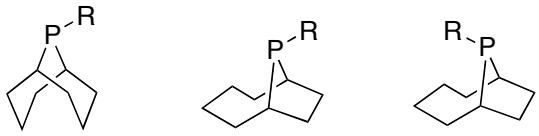

R = $CH_2CH_2CH_2CH_3$	*s*-PhobP^{n}Bu	a_5-PhobP^{n}Bu	a_7-PhobP^{n}Bu
R = $CH_2CH(CH_3)_2$	*s*-PhobP^{i}Bu	a_5-PhobP^{i}Bu	a_7-PhobP^{i}Bu
R = $CH(CH_3)CH_2CH_3$	*s*-PhobP^{s}Bu	a_5-PhobP^{s}Bu	
R = $C(CH_3)_3$	*s*-PhobP^{t}Bu	a_5-PhobP^{t}Bu	a_7-PhobP^{t}Bu

Scheme 1

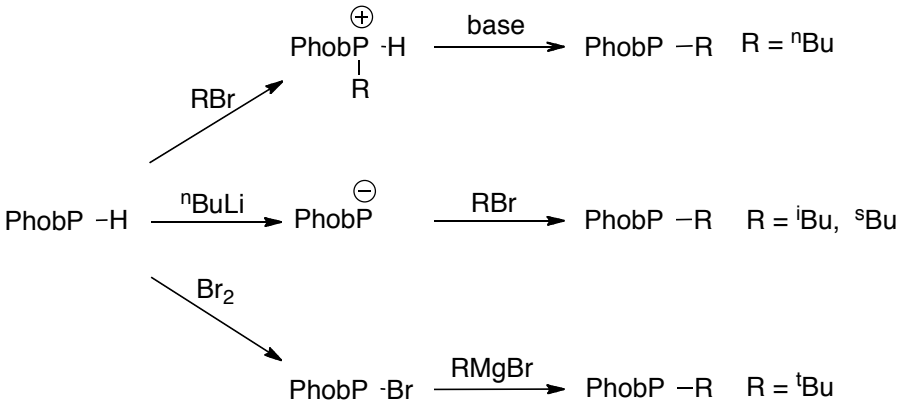

Samples of the butylphobanes shown in Chart 2 were converted to the corresponding selenides by treatment with KSeCN in MeOH and the PhobP(Se)R species were characterized by ^{31}P NMR spectroscopy and mass spectrometry. The values for J_{PSe} are collected in Table 1 and these can be used to evaluate the σ–donor properties of the ligands. Roodt et al.[9] have shown that the smaller the value of J_{PSe}, the greater the σ-donation capacity of the ligand; to calibrate the values given in Table 1, J_{PSe} values for $Cy_nPh_{3-n}P{=}Se$ are 673 Hz (n = 3), 701 Hz (n = 2) and 725 Hz (n = 1).[9] The data in Table 1 clearly show that the order of strength of σ-donation is consistently in the order $a_7 > s > a_5$. The effect of the R groups can be gauged from the J_{PSe} values for *s*- and a_5-PhobP(Se)R which are in the order ^{t}Bu > ^{i}Bu > ^{n}Bu > ^{s}Bu; the anomalous position of ^{s}Bu in this series shows that the order is not simply the product of inductive effects of the R groups.

The crystal structures of the three diastereoisomers of PhobP(Se)^{n}Bu have been determined (Figure 1). The deviation from tetrahedral geometry at the phosphorus atom (C-P-C angle) is significant and most pronounced in the *asym* isomers. The conformations of the *n*-butyl substituents are quite different in the crystal structures of the three PhobP(Se)^{n}Bu isomers; the Se1-P1-C9-C10 torsion angles are 61° for the *s*, 49° for the a_5 and 45° for the a_7 isomers. This unduly influences the crystallographically determined cone angles for the three ligands but if the cone angles are determined by encompassing only the C9 atoms of the n-butyl groups, the values are 158° (*s*), 160° (a_5) and 149° (a_7) giving the expected[1] order of steric bulk of $a_5 > s > a_7$.

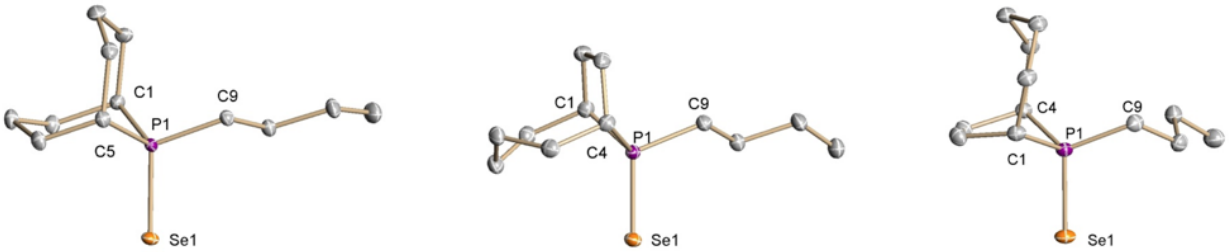

(a) (b) (c)

Figure 1. Crystal structures of the isomers of PhobP(Se)^{n}Bu (hydrogen atoms omitted for clarity). Selected bond lengths (Å) and angles (°): (a) *s*-PhobP(Se)^{n}Bu: Se(1)-P(1), 2.1313(4); C(1)-P(1)-C(5), 97.22(4); (b) a_5-PhobP(Se)^{n}Bu: Se(1)-P(1), 2.1196(4); C(1)-P(1)-C(4), 94.04(6); (c) a_7-PhobP(Se)^{n}Bu: Se(1)-P(1), 2.1259(5); C(1)-P(1)-C(4), 93.63(9).

Table 1. Values of J_{PSe} for PhobP(Se)R[a]

R	J_{PSe} / Hz		
	s-PhobP(Se)R	a_5-PhobP(Se)R	a_7-PhobP(Se)R
^{n}Bu	684	707	662
^{i}Bu	679	703	*b*
^{s}Bu	688	712	*b*
^{t}Bu	678	705	648

a Spectra measured in $CDCl_3$
b Compound not observed.

Platinum(II) and palladium(II) complexes. The complexes *trans*-[$PtCl_2$(PhobPBu)$_2$] where M = Pt or Pd (Chart 3) were prepared by the addition of single diastereoisomers of PhobPBu to [$PtCl_2$(NC^{t}Bu)$_2$] or [$PdCl_2$(NCPh)$_2$]. The trans geometry of the platinum complexes in solution was assigned on the basis of the values of J_{PtP} which lie in the range 2200-2600 Hz (Table 2), typical of *trans*-[$PtCl_2$(PR_3)$_2$].[10] The trans geometry of the palladium complexes was assigned on

the basis of the observation of virtual triplets in their ^{13}C NMR spectra[11] (see Experimental for the details).

Chart 3

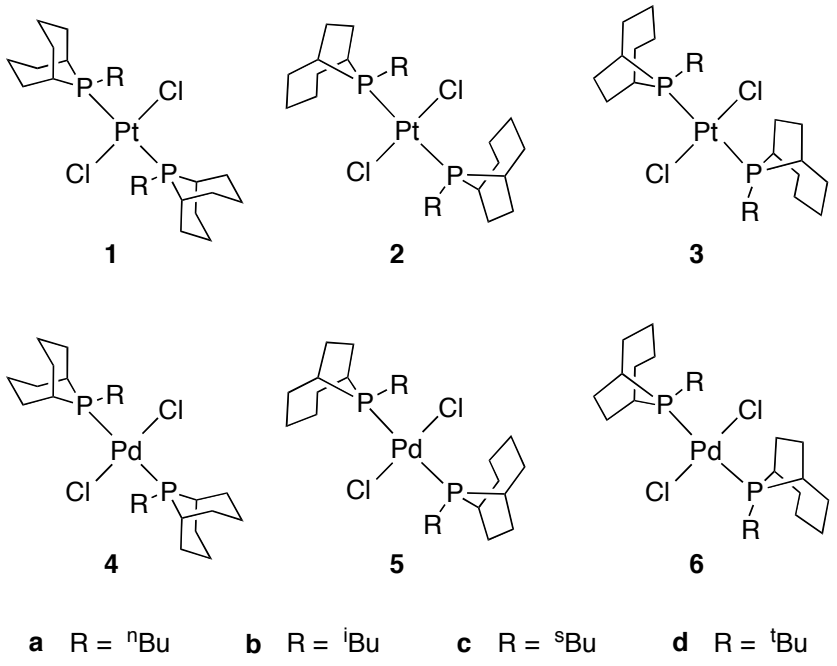

a R = ^{n}Bu **b** R = ^{i}Bu **c** R = ^{s}Bu **d** R = ^{t}Bu

Table 2. ^{31}P NMR data for complexes *trans*-[MCl_2(PhobPBu)$_2$] where M = Pt or Pd.[a]

Complex	R	δ_P / ppm	J_{PPt} / Hz	T_c / °C	$\Delta G^{\ddagger}$ / kcal mol^{-1}
1a	^{n}Bu	4.1	2437	–30	12
1b	^{i}Bu	4.2, 3.2	2502, 2502	+50	15
1c	(*R*)-^{s}Bu	9.3, 7.8	2493, 2614	+20	14
1d	^{t}Bu	19.8, 19.6	2231, 2231	>100	>19
2a	^{n}Bu	40.7	2411	-10	
2b	^{i}Bu	38.4, 37.8	2404, 2407	+70	17
3a	^{n}Bu	34.5	2311	–80	9
3b	^{i}Bu	31.6	2305	–30	12
4a	^{n}Bu	9.5		–30	11
4b	^{i}Bu	8.6, 7.2		+50	15
5a	^{n}Bu	48.1		–30	12
5b	^{i}Bu	46.2, 45.4		+60	16
6a	^{n}Bu	39.5		–100	8
6b	^{i}Bu	37.8		–50	11

a Spectra at low temperatures were measured in CD_2Cl_2 and at high temperatures were measured in $C_2D_2Cl_4$.

The crystal structures of the *n*-butylphobane complexes **1-4a** are shown in Figure 2; the structures of **1a** and **3a** were previously reported.[1] The crystal structures of the *i*-butylphobane complexes **1-6b** are shown in Figure 3. In all but two of these ten crystal structures, the R substituents are on opposite sides of the square plane (anti); the exceptions are **3b** and **6b** where the substituents are on the same side of the square plane (syn). In fact, in all but **3b** and **6b**, the metal atom sits on an inversion centre, such that the trans phosphines are related by crystallographic inversion symmetry (i.e. torsion angle C(9)-P(1)…P(1A)-C(9A) = 180°).

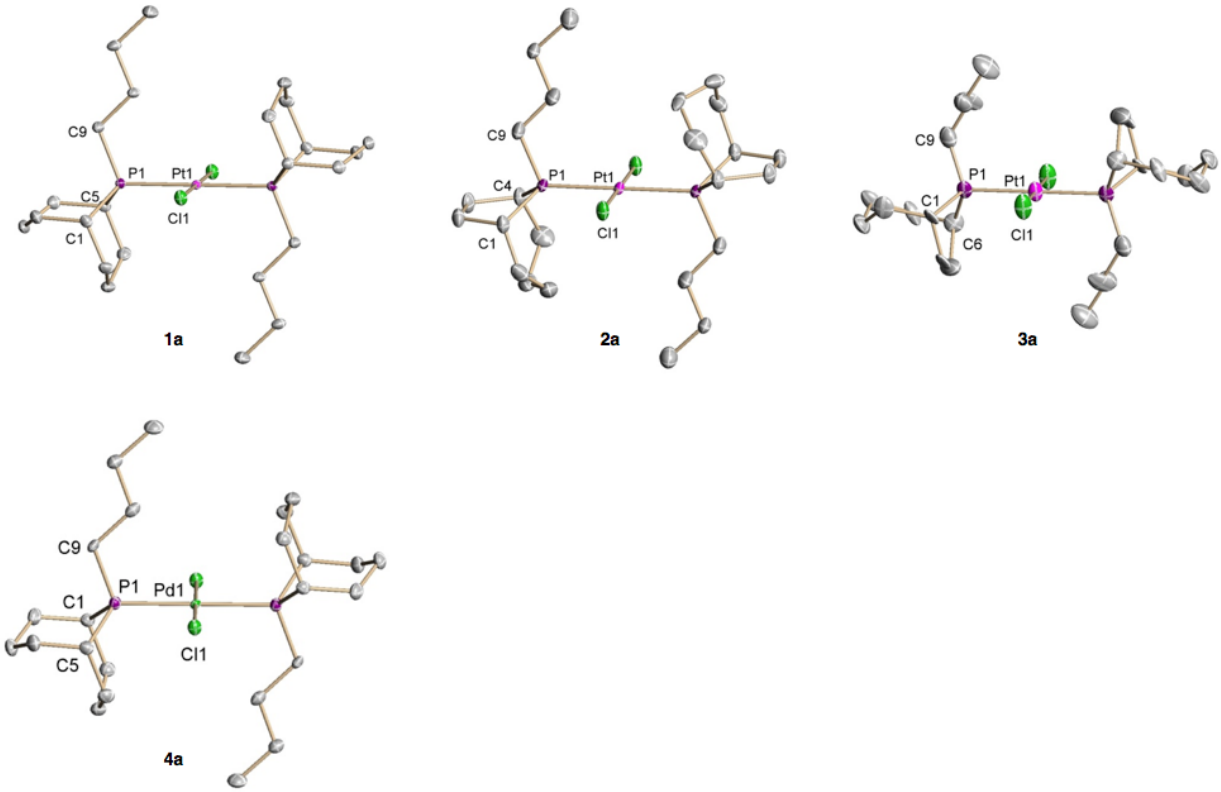

Figure 2. Crystal structures of *trans*-[MCl_2(PhobP^{n}Bu)$_2$]. All hydrogen atoms omitted for clarity. Ellipsoids drawn at 50% probability. Selected bond lengths and angles: **1a**[1]: Pt(1)-Cl(1), 2.3060(10); Pt(1)-P(1), 2.3121(10); C(1)-P(1)-C(5), 95.87(15); Cl(1)-Pt(1)-P(1)-C(9), 89.92(12);

C(9)-P(1)-P(1A)-C(9A), 180.0. **2a**: Pt(1)-Cl(1), 2.3155(16); Pt(1)-P(1), 2.3079(16); C(1)-P(1)-C(4), 93.1(3); Cl(1)-Pt(1)-P(1)-C(9), 88.8(3); C(9)-P(1)-P(1A)-C(9A), 180.0. **3a**[1]: Pt(1)-Cl(1), 2.319(4); Pt(1)-P(1), 2.321(4); C(1)-P(1)-C(6), 97.2(8); Cl(1)-Pt(1)-P(1)-C(9), 71.1(7); C(9)-P(1)-P(1A)-C(9A), 180.0; Pt(1)-P(1)-C(9)-C(10), 32(2). **4a**: Pd(1)-Cl(1), 2.3082(12); Pd(1)-P(1), 2.3221(13); C(1)-P(1)-C(5), 96.5(3); Cl(1)-Pd(1)-P(1)-C(9), -89.9(2); C(9)-P(1)-P(1A)-C(9A), 180.0.

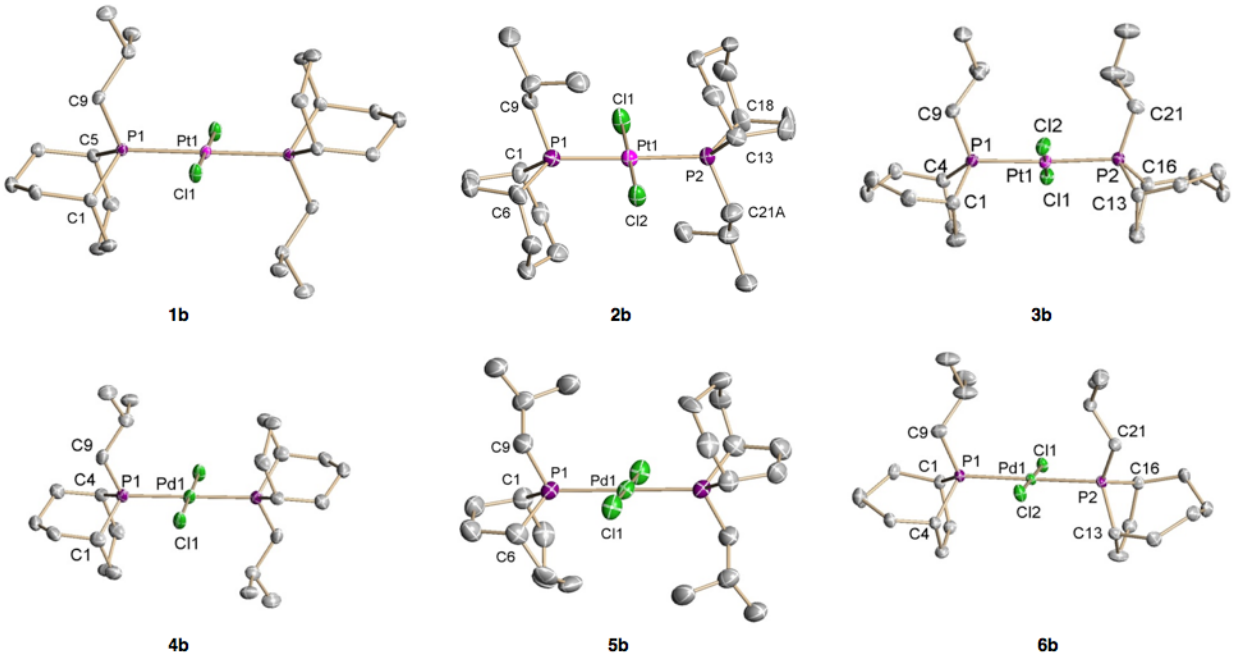

Figure 3. Crystal structures of *trans*-[$MCl_2(PhobP^iBu)_2$]. All hydrogen atoms omitted for clarity. Ellipsoids drawn at 50% probability. Selected bond lengths and angles: **1b**: Pt(1)-Cl(1), 2.3156(6); Pt(1)-P(1), 2.3133(6); C(1)-P(1)-C(5), 96.18(12); Cl(1)-Pt(1)-P(1)-C(9), 72.32(9); C(9)-P(1)-P(1A)-C(9A), 180.0. **2b**: Pt(1)-Cl(1), 2.315(2); Pt(1)-Cl(2), 2.315(2); Pt(1)-P(1), 2.311(2); Pt(1)-P(2), 2.321(2); C(1)-P(1)-C(6), 93.7(5); C(13)-P(1)-C(18), 93.4(4); Cl(1)-Pt(1)-P(1)-C(9), -71.1(4); Cl(2)-Pt(1)-P(2)-C(21A), 68.3(4); C(9)-P(1)-P(2)-C(21A), 177.3 (5). **3b**: Pt(1)-Cl(1), 2.3111(6); Pt(1)-Cl(2), 2.3208(6); Pt(1)-P(1), 2.3161(7); Pt(1)-P(2), 2.3150(7); C(1)-P(1)-C(4), 93.04(12); C(13)-P(1)-C(16), 93.33(11); Cl(1)-Pt(1)-P(1)-C(9), -121.53(10); Cl(2)-

Pt(1)-P(2)-C(21), -68.69(9); C(9)-P(1)-P(2)-C(21), -10.2(1). **4b**: Pd(1)-Cl(1), 2.3096(18); Pd(1)-P(1), 2.3232(19); C(1)-P(1)-C(5), 96.3(4); Cl(1)-Pd(1)-P(1)-C(9), -108.3(3); C(9)-P(1)-P(1A)-C(9A), 180.0. **5b**: Pd(1)-Cl(1), 2.3178(6); Pd(1)-P(1), 2.3271(7); C(1)-P(1)-C(6), 92.65(14); Cl(1)-Pd(1)-P(1)-C(9), 72.16(11); C(9)-P(1)-P(1A)-C(9A), 180.0. **6b**: Pd(1)-Cl(1), 2.3055(4); Pd(1)-Cl(2), 2.3112(4); Pd(1)-P(1), 2.3234(4); Pd(1)-P(2), 2.3263(4); C(1)-P(1)-C(4), 93.29(7); C(13)-P(1)-C(16), 93.03(7); Cl(1)-Pd(1)-P(1)-C(9), -110.73(6); Cl(2)-Pd(1)-P(2)-C(21), -58.41(6); C(9)-P(1)-P(2)-C(21), 10.68(8).

One striking feature of the ^{31}P NMR spectra for the *trans*-[MCl_2(PhobPBu)$_2$] complexes, the data for which are presented in Table 2, is that the ambient temperature spectra of some of the complexes show two sharp singlets at similar chemical shifts which coalesce at higher temperatures. Moreover, in the cases where one singlet was observed at room temperature, the low temperature ^{31}P NMR spectra also showed two singlets. This indicates that the complexes generally exist in two forms which (from the observed ratios of between 3:1 and 1:1) are close in energy and interconvert on the NMR timescale with coalescence temperatures ranging from -100 °C to over + 100 °C, which translates[12] into free energies of activation $\Delta G^{\ddagger}$ of 8 to >19 kcal mol^{-1} (see Table 2). It is proposed that the fluxionality is due to interconversion of two rotamers (Scheme 2) by slow rotation around the Pt–P bond; one of the rotamers has C_{2h}-symmetry with the R groups of the PhobPR ligands anti to each other (as in the crystal structures of **1-4a**) and the second rotamer has C_{2v}-symmetry with the R groups syn to each other (as in the crystal structures of **3b** and **6b**).

The restricted M–P rotation hypothesis is supported by DFT calculations (B3LYP/6-31G* and LACV3P on Pt) on the isomeric complexes *trans*-[$PtCl_2$(*s*-PhobPBu)$_2$] (**1a** and **1b**), which revealed two energy minima at torsion angles ϕ(C-P-P-C) = 168° and 338° for the quasi C_{2h} and

C_{2v} conformations respectively for **1a**, and ϕ(C-P-P-C) = 141° and 319° for **1b**. The rotation profiles were computed by rotating one phosphine about its Pt–P bond in 30° increments, showing a barrier to rotation between the two minima of 9.7 kcal mol^{-1} for **1a** and 15.2 kcal mol^{-1} for **1b** (see Figure 3). Despite the simplicity of these gas-phase calculations that take no account of solvation and dispersion effects,[13] these calculated values are close to the NMR-determined solution values of 12 kcal mol^{-1} for **1a** and 15 kcal mol^{-1} for **1b** (see Table 2).

Scheme 2

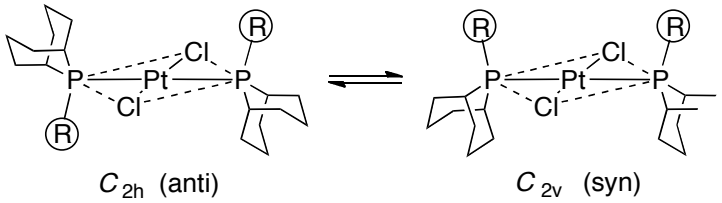

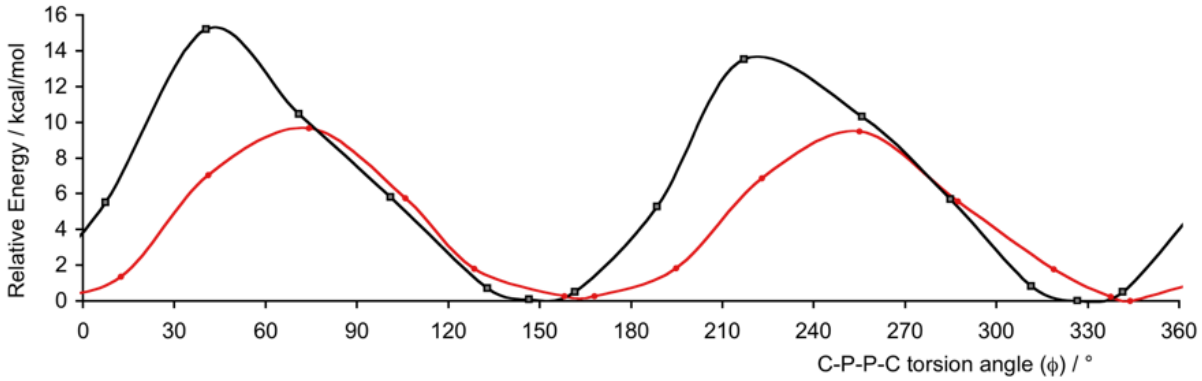

Figure 4. Pt–P rotation profiles for *trans*-[$PtCl_2$(*s*-PhobPR)$_2$] in kcal mol^{-1} relative to the energy minimum (at ϕ = 344°for **1a**, and 141° for **1b**). Complex legend: red = **1a** (R = ^{n}Bu); black = **1b** (R = ^{i}Bu).

From the energy barriers to M–P rotation obtained by NMR spectroscopy and given in Table 2, the following observations can be made. (1) The barriers for the *trans*-[$PtCl_2$(*s*-PhobPBu)$_2$] (**1a–**

d) increase in the order ^{n}Bu < ^{s}Bu ~ ^{i}Bu < ^{t}Bu. (2) The barriers are consistently 3-4 kcal mol^{-1} higher for the complexes of PhobP^{i}Bu **(1–6b)** than for the analogous complexes of PhobP^{n}Bu **(1–6a)**. (3) The values for the bicyclic diastereoisomers of *trans*-[MCl_2(PhobPBu)$_2$] are in the order $a_5 \geq s > a_7$. (4) The values are similar for analogous Pt and Pd complexes. All four observations are consistent with steric effects controlling the size of the barrier – the larger the tertiary phobane, the higher the barrier (trends (1) – (3)) and the similar radii of Pt and Pd leads to similar barriers.

Restricted M–P rotation in trans square planar complexes has been previously observed with bulky phosphine ligands or when the ligands cis to the PR_3 are bulky.[5-7] Shaw et al. reported[5] NMR evidence for restricted rotation in *trans*-[$PtCl_2$(RP^{t}Bu$_2$)$_2$] (R = H, Me, Et, ^{n}Pr, CCPh) amounting to barriers in the range 8-15 kcal mol^{-1} and associated this with the bulk of the P^{t}Bu$_2$ group. However in our systems, neither the PhobP group nor the adjacent Cl ligands can be described as especially bulky using traditional measures of steric hindrance; the averaged crystallographic cone angle for PhobP from the above structures is 107° which can be compared with 115° for P^{i}Pr$_2$ in *trans*-[$PdCl_2${$PiPr_2$($CH_2CH_2CH_2CN$)}$_2$].[14] Restricted M–P rotation has also been noted in the complex [$RuCl_2$(=CHR)(*s*-PhobPCy)$_2$] but not detected in ostensibly similar complexes such as [$RuCl_2$(=CHR)($PPhCy_2$)$_2$].[15] The observation of restricted rotation of the PhobPR ligands at ambient temperatures therefore appears to be atypical and this prompted us to explore this observation further using computational methods.

Computational Study of Energy Barriers to M–P rotations. The model chosen to probe the barrier to M–P rotation was the d^8, square planar, anionic species [$PdCl_3$(R'$_2$PR)]$^-$ (where R'$_2$P = ^{t}Bu$_2$P or PhobP) in which the ligands cis and trans to the phosphine remain constant. By rotating the $PdCl_3$ fragment about the Pd–P bond, an energy profile for each phosphine can be obtained.

The calculated rotation curves for the $[PdCl_3(^tBu_2PR)]^-$ complexes (Chart 4) are shown in Figure 5(a) where the energy is plotted against the Cl–Pd–P–R torsion angle. It is clear that the peaks occur at 90°/270° and the troughs at 0°/180°. The computed structures for the conformers of $[PdCl_3(^tBu_2PCH_3)]^-$ at the turning points in the curve are shown in Figure 5(b). For the high energy 90° conformer there is a close approach (averaging 2.5 Å) of four of the H atoms of the *t*-butyl substituents to the adjacent Cl atoms but no close interactions with the methyl substituent; by extrapolation, the bulk of the R substituent should not significantly affect the energy of the 90° conformer of $[PdCl_3(^tBu_2PR)]^-$. In the low energy 0° conformer, three H....Cl interactions (averaging 2.7 Å) are identified, one of which involves the P–CH_3 substituent; by extrapolation, the more bulky the R substituent, the higher the energy of the 0° conformer of $[PdCl_3(^tBu_2PR)]^-$ should become which would have the effect of compressing the barrier to rotation. Thus the energy barrier to Pd–P rotation in $[PdCl_3(^tBu_2PR)]^-$ is inversely correlated with the steric bulk of the R group, rising in the order ^{t}Bu < ^{i}Pr < Me < H. This is consistent with the reported highly restricted rotations in *trans*-$[PtCl_2(^tBu_2PR)_2]$ (R = H, CCPh) observed by NMR spectroscopy.[5]

Chart 4

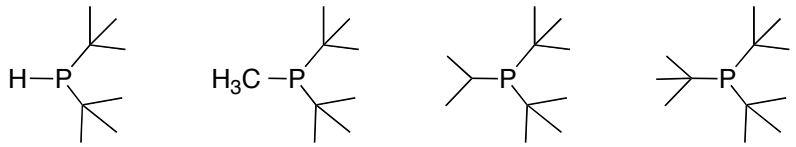

A **B** **C** **D**

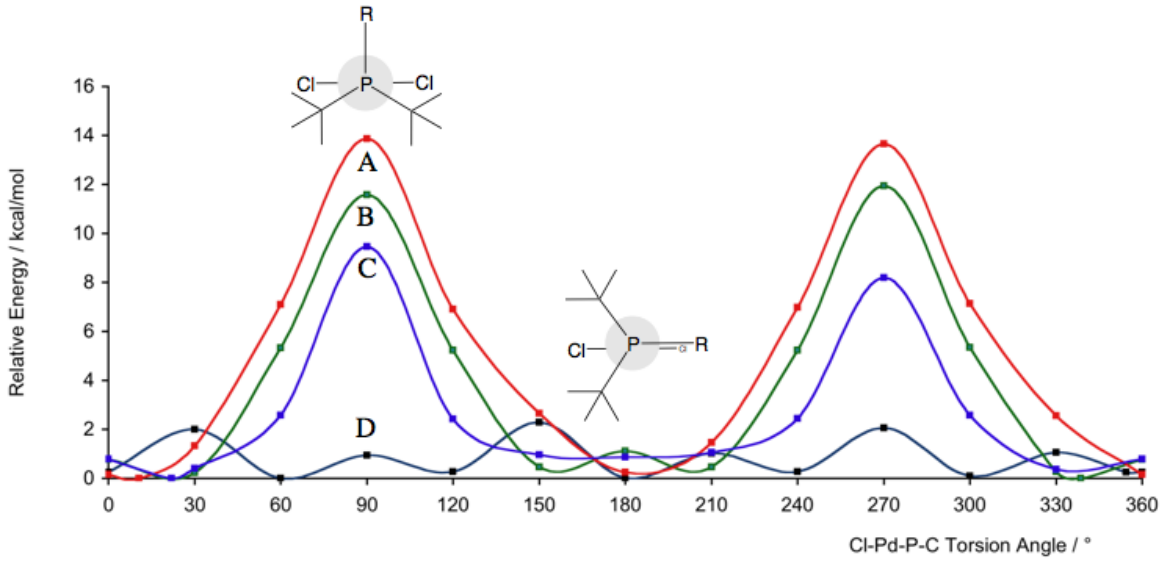

(a)

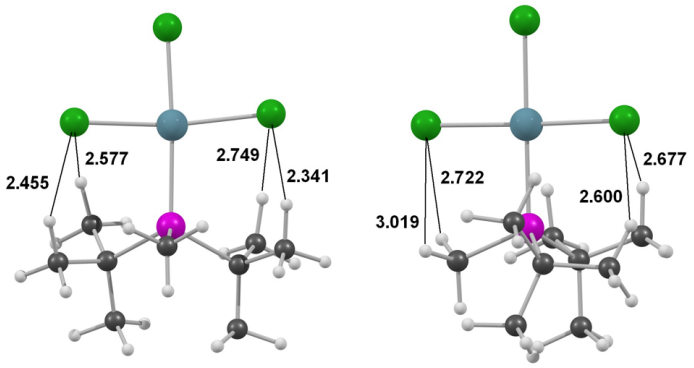

(b)

Figure 5. (a) Pd–P rotation profiles in kcal mol^{-1} relative to the energy minimum for complexes A–D (see Chart 4). Projections shown are looking down the P–Pd bond for the 90° / 270° and 0° / 180° conformers. (b) Calculated structures for the 90° and 0° conformers of $[PdCl_3(PMe^tBu_2)]^-$ with the closest Cl.....H distances (in Å) annotated.

The calculated Pd–P rotation curves for the $[PdCl_3(s\text{-PhobPR})]^-$ complexes (Chart 5) are shown in Figure 6(a) and it is apparent that the barrier to rotation increases with increasing bulk of the R group rising in the order H < Me < ^{n}Bu < ^{s}Bu < ^{i}Bu < ^{t}Bu. This parallels the order of the

barriers to rotation observed experimentally by NMR for the *trans*-[MCl_2(PhobPBu)$_2$] complexes (Table 2). In Figure 6(b), the calculated Pd–P rotation curves for the diastereoisomers of [$PdCl_3$(PhobP^{n}Bu)]$^-$ are shown and the observed trend in barriers to rotation of $a_5 \geq s > a_7$ is also the same as that observed experimentally for the diastereoisomers of *trans*-[MCl_2(PhobP^{n}Bu)$_2$] complexes (Table 2). The minima in the curves occur when the Pd–Cl and P–R are approximately orthogonal (80-110˚) which is the conformation observed in all ten of the crystal structures of the *trans*-[MCl_2(PhobPBu)$_2$] complexes described above. The results displayed in Figure 6 show that the DFT calculations on the model complex [$PdCl_3$(PhobPR)]$^-$ faithfully reproduced the trends observed by NMR for the *trans*-[MCl_2(PhobPR)$_2$] complexes.

Chart 5

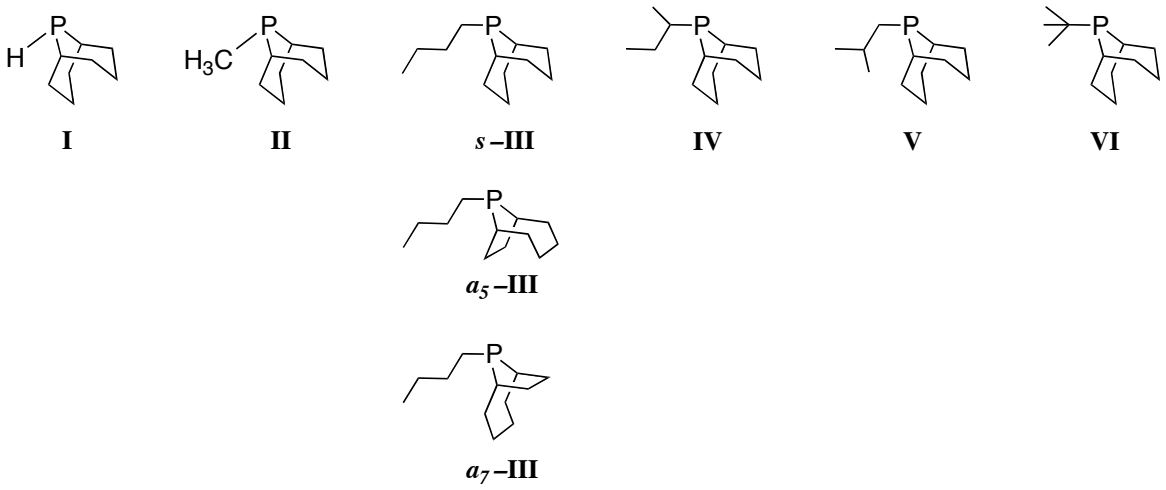

I **II** ***s*–III** **IV** **V** **VI**

***a*$_5$–III**

***a*$_7$–III**

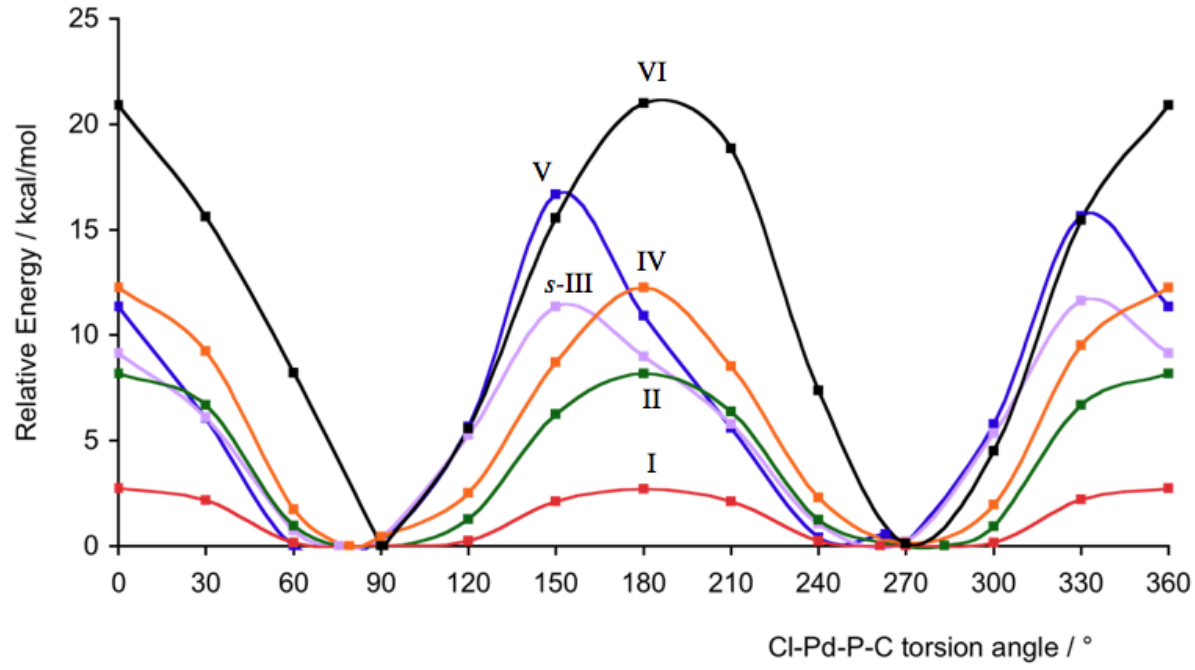

(a)

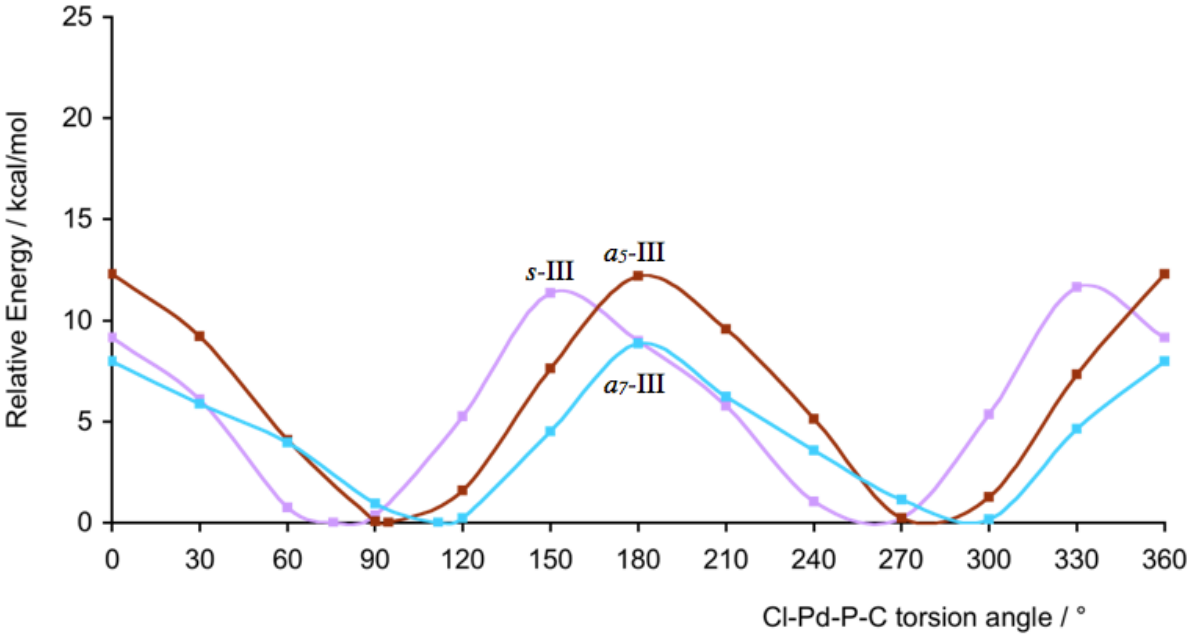

(b)

Figure 6. Pd–P rotation profiles in kcal mol^{-1} relative to the energy minimum for complexes I–VI (see Chart 5).

Scrutiny of the curves of Figure 6 shows that the minima consistently occur at Cl–Pd–P–R torsion angles in the vicinity of 90˚ and 270˚ but the maxima occur in two regions: at 0˚/180˚ for R = H, CH_3, ^{s}Bu or ^{t}Bu and at 150˚/330˚ (i.e. 150˚/-30˚) for R = ^{n}Bu, ^{i}Bu. These observations can be rationalized qualitatively in terms of steric interactions between H atoms on the phobane ligands and the adjacent M–Cl. In the low energy, 90˚ conformer of $[PdCl_3(s\text{-PhobPCH}_3)]^-$ shown in Figure 7(a), there are no short (< 3.0 Å) H…..Cl contacts identified and it can be inferred that the bulk of the R substituent would not significantly affect the energy of the 90˚ conformer. In the high energy 0˚ conformer (Figure 7(b)), there are two short 1,3-diaxial H….Cl contacts (< 2.6 Å) across the chair-like phosphacycle between a Pd–Cl and two C–H groups and there are two H….Cl contacts (< 2.9 Å) between the P–CH_3 with an Pd–Cl. The repulsive interactions identified in the 0˚ conformer of $[PdCl_3(s\text{-PhobPCH}_3)]^-$ would be expected to increase for $[PdCl_3(s\text{-PhobPR})]^-$ if the bulk of R were greater than CH_3 and this would produce an increased barrier to rotation. Thus the high rotational barrier of ca. 21 kcal mol^{-1} calculated for $[PdCl_3(s\text{-PhobP}^{t}\text{Bu})]^-$ is understandable in terms of the very close contacts between the Pd–Cl groups and two of the β-hydrogens of the t-butyl group and 1,3-diaxial hydrogens of the phosphacycle in the 0˚ conformer as shown in Figure 7(c).

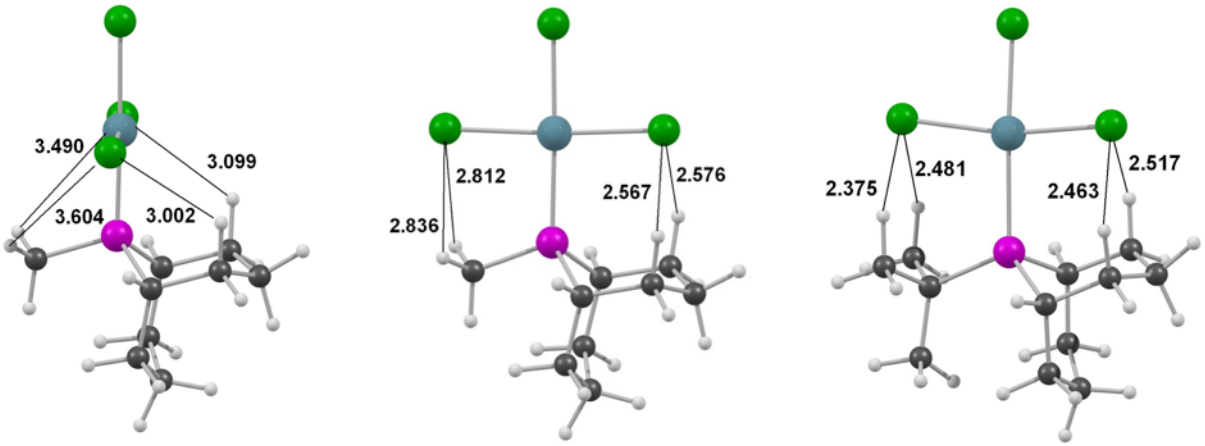

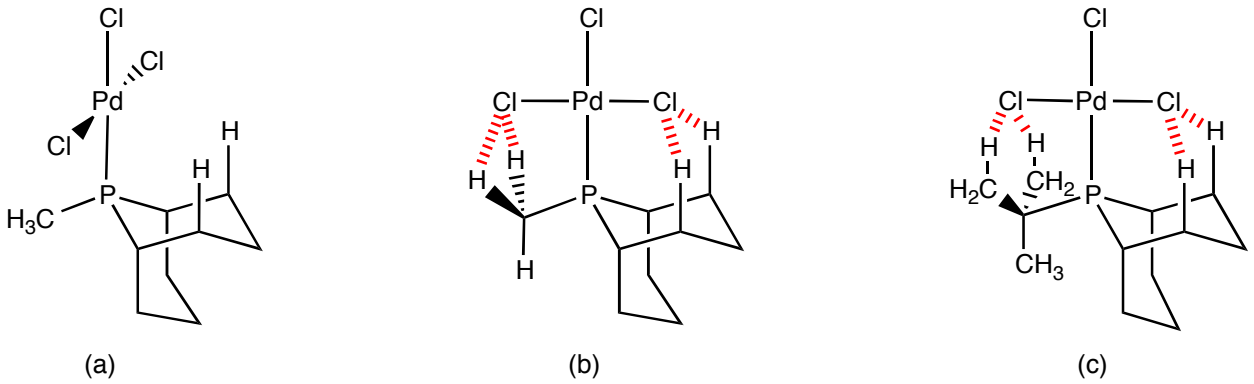

Figure 7. Computed structures of $[PdCl_3(PhobPR)]^-$ with the close Cl.....H distances (in Å) annotated for (a) $\phi = 90°/270°$, R = Me; (b) $\phi = 0°/180°$, R = Me; (c) $\phi = 0°/180°$, R = ^{t}Bu.

It is more difficult to be definitive about the steric interactions that determine the Pd–P rotation profiles for other *s*-PhobPR ligands because these will depend on the conformation of the chain in the substituent R group which can potentially adopt several conformations of similar energy; for example, the ^{n}Bu chain adopts three different conformations in the diastereoisomers of PhobP(=Se)^{n}Bu (see Figure 1). Nevertheless, it is instructive to examine the source of the large calculated rotational barriers for $[PdCl_3(s\text{-PhobPR})]^-$ of 12 (R = ^{n}Bu) and 17 (R = ^{i}Bu) kcal mol^{-1} and the 30° shift in the position of the energy maxima relative to $[PdCl_3(s\text{-PhobPMe})]^-$ (see Figure 6(a). The complex $[PdCl_3(s\text{-PhobP}^i\text{Bu})]^-$ was selected for further study because the conformational analysis for the $PCH_2CH(CH_3)_2$ substituent is relatively simple. For the favored conformation of the isobutyl substituent, a Cl–Pd–P–C of 0° produces Pd–Cl interactions with an H atom on each of the α-C and β-C of the isobutyl group in addition to interactions with two axial H atoms in the phosphacycle (Figure 8(a)). Rotation of the $PdCl_3$ through 30° produces two very short H....Cl contacts (< 2.4 Å): one with a β-C–H of the isobutyl group and the other with an axial C–H in the bicycle (Figure 8(b)). It is the repulsive energy of these interactions that is the likely explanation for the 30° translocation and the higher energy of the peaks in the rotation profile for $[PdCl_3(s\text{-PhobP}^i\text{Bu})]^-$ relative to those for $[PdCl_3(s\text{-PhobPMe})]^-$. It therefore appears

that the Pd–Cl interaction with the β-C–H is greater than with the α-C–H in these complexes. Once again, all of these H….Cl interactions are minimized in the 90˚ conformer.

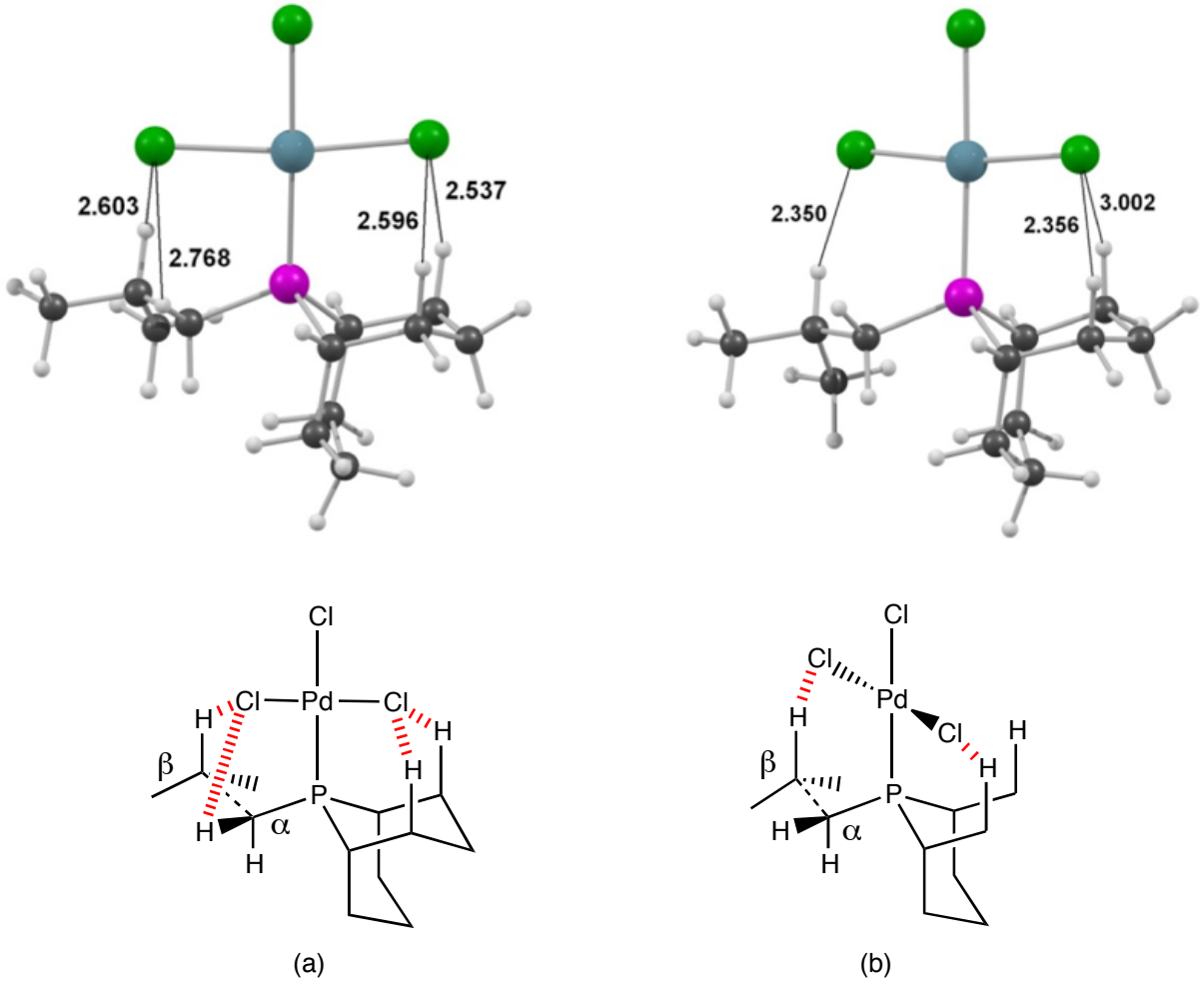

Figure 8. Computed structures of $[PdCl_3(PhobP^iBu)]^-$ with the close Cl.....H distances (in Å) annotated when (a) ϕ = 0°/180˚; (b) ϕ = 150˚/330° (–30˚).

The central inference from the DFT conformational studies is that the rigidity of the bicycle in the PhobPR ligands leads to unavoidable clashes between axial H atoms in the bicycle and the cis Cl ligands resulting in high barriers to M–P rotation. The barriers to M–P rotation in the PhobPR complexes are larger than any previously reported.

Conclusion

Prior to this work, restricted M–P rotation had been identified as an important characteristic of the coordination chemistry of $^{t}Bu_2PR$ ligands.[6] Complexes of $^{t}Bu_2PR$ ligands have found widespread applications in homogeneous catalysis ranging from C–X coupling reactions[7,16] to ethene methoxycarbonylation.[17] The conformational rigidity of $^{t}Bu_2PR$ complexes partly explains their facility to undergo cyclometallation,[6] and this feature has been exploited notably in the burgeoning area of pincer complexes derived from ligands featuring $^{t}Bu_2P$ groups.[18] Here we have shown that complexes of the bicyclic phosphines PhobPR, which are not deemed to be bulky, also exhibit restricted M–P rotation.

From NMR measurements on *trans*-$[MCl_2(R'_2PR)_2]$ (M = Pd, Pt; R'_2P = $^{t}Bu_2P$ or PhobP) and computational studies on the model complexes $[PdCl_3(R'PR_2)]^-$, the barriers to rotation depend on the bulk of substituent R. However the trend in the energy barriers depends on R'_2P: for $^{t}Bu_2PR$ complexes, the barrier increases with decreasing size of R but for PhobPR the barrier increases with increasing size of R (see Figure 9(a)). The corollary of these trends is that the barriers to M–P rotation for square planar complexes with trans $^{t}Bu_2PR$ ligands reach a natural maximum for R = H whereas the barrier for the analogous PhobPR complexes does not have such a limitation. This releases scope for the design of PhobPR ligands whose complexes may have still higher barriers to rotation than those reported here.

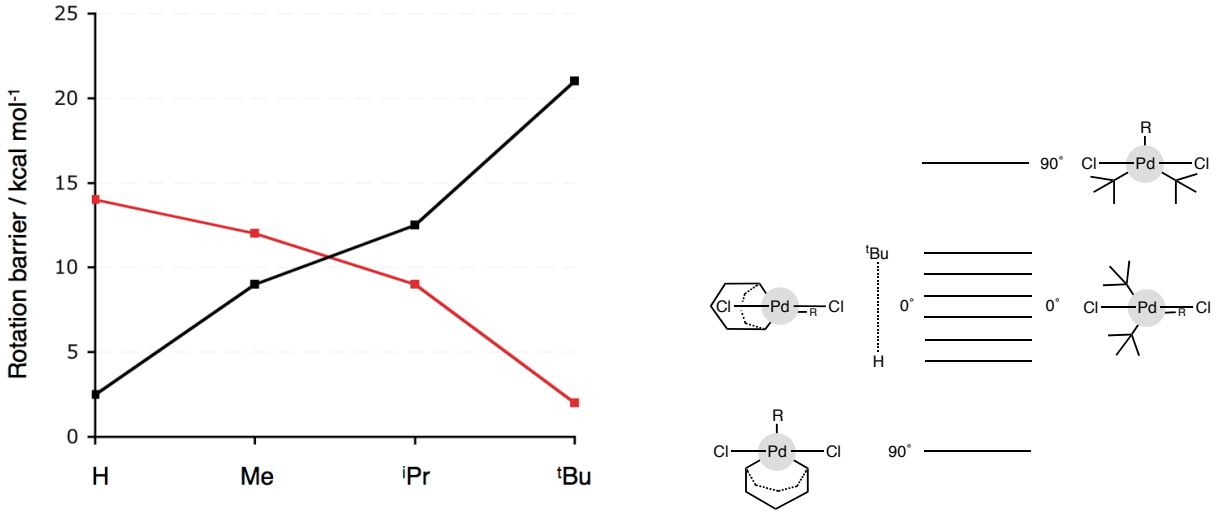

(a) (b)

Figure 9. (a) Calculated barriers to M–P rotation as a function of R substituent in the model complexes $[PdCl_3(R'_2PR)_2]^-$ where R'_2P = $^tBu_2P$ (red) or PhobP (black). (b) Schematic representation of the conformer energies for the complexes $[R'_2PR–PdCl_3]^-$ where R'_2P = PhobP and $^tBu_2P$.

The diagram in Figure 9(b) can be used to explain succinctly the contrasting effects the bulk of the R groups have on the barrier to Pd–P rotation in the square planar complexes $[R'_2PR–PdCl_3]^-$ where R'_2P = PhobP and $^tBu_2P$. For all of the complexes of $^tBu_2PR$ and most of the complexes of PhobPR, the R group will have its greatest effect on the energy when the P–R eclipses the Pd–Cl (the 0˚ conformer) ranging from R = H (lowest) to R = ^{t}Bu in Figure 9(b). When the P–R is orthogonal to the Pd–Cl (the 90˚ conformer), the effect of the R group will be negligible. For the $^tBu_2PR$ complexes, the energy is dominated by the repulsive interactions of Pd–Cl with the two bulky ^{t}Bu substituents which are a maximum for the 90˚ conformer and therefore, as is clear from Figure 9(b), the greater the bulk of R, the more compressed the energy separation is between the rotamers. By contrast, for the PhobPR complexes, the energy is a function of the repulsive 1,3-diaxial interactions of Pd–Cl with the phosphacycle C–H groups (see above) which are a

minimum for the 90° conformer and therefore, as is clear from Figure 9(b), the greater the bulk of R, the greater the energy separation is between the rotamers. These conclusions should be general for square planar complexes of PhobPR ligands.

The rigidity (or preoganisation) of coordinated $^{t}Bu_2PR$ ligands has well-documented consequences for the chemistry of their complexes and may well be a component in the success of $^{t}Bu_2PR$ ligands in catalysis. The ramifications of the high rigidity of coordinated PhobPR ligands for their chemistry are currently under investigation.

Experimental

General considerations. Unless otherwise stated, all work was carried out under a dry nitrogen atmosphere, using standard Schlenk line techniques. Dry N_2-saturated solvents were collected from a Grubbs system[19] in flame and vacuum dried glassware. The complexes $[PtCl_2(NC^{t}Bu)_2]$[20] and $[PdCl_2(NCPh)_2]$[21] were made by literature methods. Isomeric mixtures of phobanes were obtained from Shell or Rhodia and the following phobanes were made by our previously published methods:[1] *s*-PhobPCl, *s*-PhobP^{n}Bu, a_5-PhobP^{n}Bu, a_7-PhobP^{n}Bu. All other chemicals were purchased from Aldrich. NMR spectra were measured on a Jeol ECP 300, Lambda 300, ECP 400 or Varian 400. Unless otherwise stated, ^{1}H, ^{13}C, ^{31}P and ^{19}F NMR spectra were recorded at 400, 100, 121 and 282 MHz respectively at +23 °C. Mass spectra were recorded on a VG Analytical Autospec or Bruker Daltonics Apex IV spectrometer. Elemental analyses were carried out by the Microanalytical Laboratory of the School of Chemistry, University of Bristol.

Preparation of *s*-PhobPBr. Pure *s*-PhobPH (5.00 g, 35.2 mmol) was dissolved in CH_2Cl_2 (50 cm^3). A solution of Br_2 (1.81 cm^3, 35.2 mmol) in CH_2Cl_2 (50 cm^3) was added at 0 ºC over 2 h. The solution was filtered and the solvent was removed under reduced pressure to give *s*-PhobPBr

(6.20 g, 28.0 mmol, 80%). The product was then redissolved in toluene (50 cm^3) and used as a stock solution (0.56 M). ^{31}P NMR (C_6D_6): δ_P 91.4. ^{13}C NMR ($CDCl_3$): δ_C 31.3 (d, J_{PC} 17.1 Hz), 29.7 (d, J_{PC} 31.1 Hz), 25.3 (d, J_{PC} 3.9 Hz), 22.5 (d, J_{PC} 3.1 Hz), 21.3 (s). ^1H NMR ($CDCl_3$): δ_H 2.65 (2H, br s), 2.51 (2H, br s), 2.20 (4H, br m), 2.09-1.60 (6H, m), 1.57 (1H, m), 1.42 (1H, m). HRMS (EI): calcd. for $C_8H_{14}BrP$: 220.0017, found, 220.0009.

Preparation of *s*/*a*-mixture of PhobPBr. The phobane mixture (10 cm^3 in toluene) was concentrated under reduced pressure and the resultant PhobPH (7.20 g, 52.0 mmol) was then dissolved in CH_2Cl_2 (100 cm^3). A solution of Br_2 (3.0 cm^3, 58 mmol) in CH_2Cl_2 (100 cm^3) was added at 0 ºC over 3.5 h. The reaction was monitored by ^{31}P NMR spectroscopy which showed how the starting material PhobPH was converted to PhobPBr through several intermediate species. When the reaction was complete, some white solid, probably $PhobPBr_3$, had precipitated from solution (< 0.2 g). The solution was filtered and the solvent was removed under reduced pressure to give PhobPBr (9.00 g, 40.7 mmol, 78%). The product was redissolved in hexane or toluene and used as a stock solution or further purified by distillation (74-76 ºC at 0.41 mmHg) affording a clear liquid. ^{31}P NMR (C_6D_6): δ_P *s* 91.4, *a* 130.0.

Preparation of *s*-PhobP^{i}Bu. Pure *s*-PhobPH (0.70 g, 4.9 mmol) was dissolved in hexane (10 cm^3) and the solution cooled to 0 °C. A solution of ^{n}BuLi (3.4 cm^3, 1.6 M in hexane, 5.4 mmol) was added dropwise over 5 min and then immediately afterwards, the solution was cooled to -78 °C and 1-bromo-2-methylpropane (0.53 cm^3, 4.9 mmol) was added dropwise over 10 min. The reaction mixture was allowed to warm to room temperature and stirred for 20 h. The solvent was then removed under reduced pressure and the residue was suspended in deoxygenated water (10 cm^3) and extracted with hexane (3 x 10 cm^3). The combined organic layers were dried over $MgSO_4$, filtered, the solvent removed under reduced pressure and the resultant product distilled

(76-78 °C at 0.56 mmHg) to give *s*-PhobP^{i}Bu as a clear liquid. Yield: 0.39 g (2.0 mmol, 40%). ^{31}P NMR (C_6D_6): δ_P, -39.3. ^{13}C NMR (C_6D_6): δ_C, 32.0 (d, J_{PC} 23.4 Hz), 31.4 (d, J_{PC} 12.5 Hz), 26.0 (d, J_{PC} 18.7 Hz), (d, J_{PC} 11.5 Hz), 23.9 (d, J_{PC} 10.9 Hz), 23.6 (d, J_{PC} 3.9 Hz), 23.2 (d, J_{PC} 9.3 Hz), 22.7 (d, J_{PC} 5.4 Hz), 20.9 (d, J_{PC} 1.6 Hz). ^{1}H NMR (C_6D_6): δ_H, 1.99-1.50 (10H, m), 1.39 (5H, br s), 1.19 (2H, d), 0.81 (6H, d). HRMS (EI): calcd. for $C_{12}H_{23}P$: 198.1537, found, 198.1534.

Preparation of *a*$_5$-PhobP^{i}Bu. Pure *a*-PhobPH (3.00 g, 21.1 mmol) was dissolved in THF (25 cm^3) and the solution cooled to 0 °C. A solution of ^{n}BuLi (14.5 cm^3, 1.6M in hexane, 23.2 mmol) was added dropwise over 15 min. The solution was stirred for 30 min and then cooled to -78 °C. 1-bromo-2-methylpropane (2.29 cm^3, 21.1 mmol) was added dropwise over 5 min and the reaction mixture was allowed to warm to room temperature and then stirred for a further 2.5 h. The solvent was then removed under reduced pressure. The residue was suspended in water (40 cm^3) and then extracted with hexane (4 x 40 cm^3). The combined organic layers were dried over $MgSO_4$. The solvent was removed under reduced pressure and the liquid product was distilled (120 °C at 1.3 mmHg) to give *a*$_5$-PhobP^{i}Bu as a clear liquid. Yield: 3.50 g (17.6 mmol, 84%, containing 4% *a*$_7$-PhobP^{i}Bu). ^{31}P{^{1}H} NMR (C_6D_6): δ_P -3.16. ^{13}C{^{1}H} NMR (CD_2Cl_2): δ_C 40.0 (d, J_{PC} 12.5 Hz), 35.3 (d, J_{PC} 15.6 Hz), 34.6 (d, J_{PC} 18.7 Hz), 33.9 (d, J_{PC} 6.23 Hz), 33.2 (d, J_{PC} 5.45), 27.3 (d, J_{PC} 16.4 Hz), 25.6 (s), 25.6 (s), 24.0 (d, J_{PC} 9.34 Hz). ^{1}H NMR (CD_2Cl_2): δ_H 2.19-2.06 (4H, m), 1.81-1.67 (2H, m), 1.66-1.60 (3H, br m), 1.50-1.28 (7H, br m), 1.02 (2H, dd), 0.96 (6H, d). Anal. Calcd for $C_{12}H_{23}P$: C, 72.69; H, 11.69. Found C, 72.26 ; H, 11.26 MS (EI): *m/z* 199.1 $(M)^+$.

Preparation of *a*$_7$-PhobP^{i}Bu. Pure *a*-PhobPH (2.00 g, 14.1 mmol) and 1-bromo-2-methylpropane (3.26 cm^3, 30 mmol) were dissolved in MeCN (5 cm^3) and the reaction mixture was heated to reflux for 96 h. The solvent was then removed under reduced pressure and the

resultant colorless precipitate suspended in diethyl ether (20 cm^3) and NaOH (15.5 cm^3 of a 1M aqueous solution, 15.5 mmol) was added. The reaction mixture was stirred for 30 min after which the two phases were separated. The aqueous phase was extracted with diethyl ether (3 x 20 cm^3). The combined washings were dried over $MgSO_4$, filtered and then concentrated under reduced pressure. The liquid product was distilled (140 °C at 1.3 mmHg) to give a_7-PhobP^{i}Bu as a clear liquid. Yield: 1.00 g (5.05 mmol, 36%, containing 8% a_5-PhobP^{i}Bu). $^{31}P\{^1H\}$ NMR (C_6D_6): δ_P -4.11. $^{13}C\{^1H\}$ NMR (CD_2Cl_2): δ_C 40.0 (d, J_{PC} 12.5 Hz), 34.5 (d, J_{PC} 10.9 Hz), 33.2 (d, J_{PC} 5.45 Hz), 30.7 (d, J_{PC} 20.2 Hz), 29.7 (d, J_{PC} 27.3 Hz), 28.8 (d, J_{PC} 22.6 Hz), 25.7 (s), 23.7 (d, J_{PC} 10.1 Hz). ^1H NMR (CD_2Cl_2): δ_H 2.33 (2H, br d), 2.04 (2H, br m), 1.80 (2H, m), 1.66 (4H, br m), 1.52 (2H, m), 1.39 (5H, br m), 0.99 (6H, d). Anal. Calcd for $C_{12}H_{23}P$: C, 72.69; H, 11.69. Found C, 72.92 ; H, 11.42. MS (EI): *m/z* 199.1 $(M)^+$.

Preparation of s/*a*-mixture of PhobP^{i}Bu. The phobane mixture (24 cm^3 in toluene) was concentrated under reduced pressure to give solid PhobPH (16.0 g, 113 mmol). This was dissolved in THF (75 cm^3) and then cooled to 0 °C. A solution of ^{n}BuLi (77.5 cm^3, 1.6M in hexane, 124 mmol) was added dropwise over 30 min and then immediately after this addition the reaction mixture was cooled to -78 °C and 1-bromo-2-methylpropane (12.3 cm^3, 113 mmol) was added dropwise over 15 min. The reaction mixture was allowed to warm to room temperature and then stirred for a further 20 h. The solvent was removed under reduced pressure and the residue was suspended in deoxygenated water (40 cm^3) and then extracted with hexane (3 x 40 cm^3). The combined organic layers were dried over $MgSO_4$, filtered and the solvent was removed under reduced pressure. The resulting product was distilled (96-98 °C at 1.4 mmHg) to give a clear liquid. Yield: 14.2 g (71.7 mmol, 64%; ratio of isomers: 61% *s*, 39% a_5). ^{31}P NMR (121 MHz, C_6D_6): δ_P *s* -39.3; a_5 -3.0; a_7 not observed.

Preparation of *s*-PhobP^{s}Bu. Pure *s*-PhobPH (1.00 g, 7.00 mmol) was dissolved in THF (10 cm^3) and then cooled to 0 °C. A solution of ^{n}BuLi (4.85 cm^3, 1.6 M in hexane, 7.70 mmol) was added dropwise over 5 min. The solution was stirred for 20 min and then cooled to -78 °C. 2-Bromobutane (0.77 cm^3, 7.0 mmol) was added dropwise over 5 min and the reaction mixture was allowed to warm to room temperature and then stirred for a further 20 h. The solvent was removed under reduced pressure and the residue was suspended in deoxygenated water (10 cm^3) and then extracted with hexane (3 x 10 cm^3). The combined organic layers were dried over $MgSO_4$, filtered and the solvent was removed under reduced pressure. The resulting product was distilled (74-76 °C at 0.45 mmHg) to give *s*-PhobP^{s}Bu as a clear liquid. Yield: 0.30 g (1.5 mmol, 21%). ^{31}P NMR (C_6D_6): δ_P, -23.8. ^{13}C NMR (C_6D_6): δ_C, 32.5 (d, J_{PC} 12.3 Hz), 32.3 (d, J_{PC} 11.5 Hz), 26.7 (d, J_{PC} 18.5 Hz), 25.4 (d, J_{PC} 19.2 Hz), 24.9 (d, J_{PC} 3.8 Hz), 24.5 (d, J_{PC} 3.8 Hz), 23.8 (d, J_{PC} 5.4 Hz), 23.5 (d, J_{PC} 28.4 Hz), 23.3 (d, J_{PC} 28.4 Hz), 21.9 (d, J_{PC} 1.5 Hz), 14.0 (d, J_{PC} 18.5 Hz), 11.7 (d, J_{PC} 10.8 Hz). ^{1}H NMR (C_6D_6): δ_H, 2.22-2.07 (2H, m), 2.02-1.75 (8H, m), 1.72 (1H, br s), 1.62-1.42 (5H, m), 1.33-1.21 (1H, m), 0.98 (3H, dd, J_{PH} 14 Hz, J_{HH} 7.3 Hz), 0.95 (3H, t). HRMS (EI): calcd. for $C_{12}H_{23}P$: 198.1537, found, 198.1531.

Preparation of *s*/*a*-mixture of PhobP^{s}Bu. The phobane mixture (30 cm^3 in toluene) was concentrated under reduced pressure to give PhobPH (20.0 g, 141 mmol). This was dissolved in THF (120 cm^3) and then cooled to 0 °C. A solution of ^{n}BuLi (97.0 cm^3, 1.6 M in hexane, 155 mmol) was added dropwise over 30 min. Once the addition was complete, the mixture was cooled to -78 °C and 2-bromobutane (15.4 cm^3, 141 mmol) was added dropwise over 15 min. The reaction mixture was allowed to warm to room temperature and then stirred for 15 h. The solvent was removed under reduced pressure and the residue was suspended in deoxygenated water (100 cm^3) and then extracted with hexane (3 x 100 cm^3). The combined extracts were dried over $MgSO_4$, filtered and the solvent was removed under reduced pressure. The resulting product was

distilled (102-104 °C at 1.9 mmHg) to give a clear liquid: Yield: 12.0 g (43%; ratio of isomers: 65% *s*, 35% a_5). ^{31}P NMR (C_6D_6): δ_P, *s* -23.8; a_5 14.5; a_7 not observed.

Preparation of *s*-PhobP-(*R*)-^{s}Bu

Pure *s*-PhobPH (13.0 g, 91.5 mmol) was dissolved in THF (15 cm^3) and the solution cooled to 0 °C. BH_3.THF (10.5 cm^3, 1 M in THF, 10.5 mmol) was added dropwise over 10 min and the mixture stirred at 0 °C for 30 min. A solution of ^{n}BuLi (6.59 cm^3, 1.6 M in hexane, 10.5 mmol) was added dropwise over 10 min. The mixture was stirred for a further 10 min and then cooled to -78 °C. (*S*)-(+)-2-butyl tosylate[22] (1.61 g, 7.03 mmol) in THF (10 cm^3) was added dropwise over 5 min and the reaction mixture was allowed to warm to room temperature and stirred for a further 3 h. The solvent was removed under reduced pressure and then pyrrolidine (15 mL) was added and the mixture stirred for 16 h. The pyrrolidine was then removed under reduced pressure and the residue was suspended in water (40 cm^3) and then extracted with hexane (4 x 40 mL). The combined organic layers were dried over $MgSO_4$. The solvent was removed under reduced pressure and the liquid residue was distilled (120 °C at 1.3 mmHg) to give *s*-PhobP^{s}Bu as a clear liquid. Yield: 3.37 g (17.0 mmol, 81%). ^{31}P{^{1}H} NMR (121 MHz, C_6D_6): δ_P -24.2. ^{1}H NMR (400 MHz, C_6D_6): δ_H 2.22-2.07 (2H, m), 2.02-1.75 (8H, m), 1.72 (1H, br s), 1.62-1.42 (5H, m), 1.33-1.21 (1H, m), 0.98 (3H, dd, J_{PH} 14.0 Hz, J_{HH} 7.3 Hz), 0.95 (3H, t, J_{HH} 14.2 Hz). ^{13}C{^{1}H} NMR (100 MHz, C_6D_6): δ_C 32.5 (d, J_{PC} 12.3 Hz), 32.3 (d, J_{PC} 11.5 Hz), 26.7 (d, J_{PC} 18.5 Hz), 25.4 (d, J_{PC} 19.2 Hz), 24.9 (d, J_{PC} 3.8 Hz), 24.5 (d, J_{PC} 3.8 Hz), 23.8 (d, J_{PC} 5.4 Hz), 23.5 (d, J_{PC} 28.4 Hz), 23.3 (d, J_{PC} 28.4 Hz), 21.9 (d, J_{PC} 1.5 Hz), 14.0 (d, J_{PC} 18.5 Hz), 11.7 (d, J_{PC} 10.8 Hz). Anal. Calcd for $C_{12}H_{23}P$: C, 72.69; H, 11.69. Found C, 72.42; H, 11.33.

Preparation of *s*-PhobP^{t}Bu. A solution of *tert*-butylmagnesium chloride (5.0 cm^3, 1.0M in THF, 5.0 mmol) was added dropwise over 10 min at 60 °C to a solution of pure *s*-PhobPBr (1.00

g, 4.50 mmol) in toluene (10 cm^3) and the mixture stirred for 3 h. The solvent was removed under reduced pressure and a saturated aqueous solution of NH_4Cl (10 cm^3) was added to it, followed by extraction with hexane (3 x 10 cm^3). The combined organic layers were dried over $MgSO_4$, filtered and the solvent was removed under reduced pressure. The resulting product was distilled (71-73 °C at 0.44 mmHg) to give *s*-PhobP^{t}Bu as a clear liquid. Yield: 0.10 g (0.50 mmol, 11%). ^{31}P NMR (C_6D_6): δ_P, -3.7. ^{13}C NMR (C_6D_6): δ_C, 34.6 (d, J_{PC} 15.4 Hz), 30.3 (d, J_{PC} 16.1 Hz), 29.3 (d, J_{PC} 13.1 Hz), 25.4 (d, J_{PC} 3.8 Hz), 24.9 (d, J_{PC} 19.2 Hz), 23.8 (d, J_{PC} 5.4 Hz), 21.6 (s). ^{1}H NMR (C_6D_6): δ_H, 2.36-2.08 (4H, m), 2.02-1.81 (6H, m), 1.62-1.51 (4H, m), 1.15 (9H, d, J_{PH} 12 Hz). MS (EI): m/z = 215 (M + O).

Preparation of *s*/*a*-mixture of PhobP^{t}Bu. A solution of *tert*-butylmagnesium chloride (88 cm^3, 0.5M in THF, 44 mmol) was added dropwise over 30 min at 60 °C to a solution of *s*/*a*-PhobPBr (9.0 g, 40 mmol) in toluene (55 cm^3) and the mixture stirred for 3 h. After 45 min, the ^{31}P{^{1}H} NMR spectrum showed a mixture of desired product (30%) and PhobP-PPhob[23] (60%). The solvent was removed under reduced pressure and then a saturated aqueous solution of NH_4Cl (30 cm^3) was added to the residue, followed by extraction with hexane (3 x 30 cm^3). The combined organic layers were dried over $MgSO_4$, filtered and the solvent was removed under reduced pressure. The resulting product was distilled (76-78 °C at 0.84 mmHg) to give a clear liquid. Yield: 1.00 g (5.05 mmol, 13%; ratio of isomers: 64% *s*, 8% a_7, 28% a_5). ^{31}P NMR (C_6D_6): δ_P, *s* -3.7; a_7 27.2; a_5 33.4.

Preparation of isomers of PhobP(=Se)^{n}Bu. Pure *s*-, a_5- or a_7-isomer of PhobP^{n}Bu (0.049 g, 0.25 mmol) was placed in an NMR tube under N_2 and then KSeCN (0.070 g, 0.50 mmol) in MeOH (0.7 cm^3) was added and the tube shaken a few times. The reactions were complete after 10 min (as shown by ^{31}P NMR spectroscopy). The solvent was removed under reduced pressure

and the solid residue was extracted with $CHCl_3$ (2 x 0.5 cm^3). Slow evaporation of the chloroform gave the desired compounds as white crystalline solids. ***s*-PhobP(=Se)^{n}Bu**: ^{31}P NMR (MeOH): δ_P, 37.2 (s, J_{PSe} 671 Hz); ($CDCl_3$): δ_P, 35.4 (s, J_{PSe} 684 Hz). ^{13}C NMR ($CDCl_3$): δ_C, 30.4 (d, J_{PC} 36.6 Hz), 27.7 (d, J_{PC} 4.7 Hz), 27.1 (d, J_{PC} 2.3 Hz), 26.3 (d, J_{PC} 42.8 Hz), 24.2 (d, J_{PC} 3.1 Hz), 23.8 (d, J_{PC} 15.6 Hz), 21.7 (d, J_{PC} 6.2 Hz), 20.5 (d, J_{PC} 6.2 Hz), 13.8 (s). ^{1}H NMR ($CDCl_3$): δ_H, 2.93-2.79 (2H, br m), 2.23-1.66 (16H, m), 1.53-1.44 (2H, m), 0.97 (3H, t). MS (EI): *m*/*z*, 278.1 (M^+). ***a*$_7$-PhobP(=Se)^{n}Bu**: ^{31}P NMR (MeOH): δ_P, 60.7 (s, J_{PSe} 649 Hz); ($CDCl_3$): δ_P, 58.8 (s, J_{PSe} 662 Hz). ^{13}C NMR ($CDCl_3$): δ_C, 42.4 (d, J_{PC} 38.4 Hz), 30.6 (d, J_{PC} 3.1 Hz), 28.6 (d, J_{PC} 12.3 Hz), 26.9 (d, J_{PC} 32.3 Hz), 26.2 (d, J_{PC} 3.1 Hz), 24.8 (s), 23.9 (d, J_{PC} 14.6 Hz), 13.9 (s). ^{1}H NMR ($CDCl_3$): δ_H, 2.82-2.69 (2H, br m), 2.66-2.56 (2H, br m), 2.27-2.18 (2H, m), 1.90-1.56 (12H, m), 1.54-1.46 (2H, m), 0.96 (3H, t). MS (EI): *m*/*z*, 278.1 (M^+). ***a*$_5$-PhobP(=Se)^{n}Bu**: ^{31}P NMR (MeOH): δ_P, 60.7 (s, J_{PSe} 696 Hz); ($CDCl_3$): δ_P, 59.4 (s, J_{Pse} 707 Hz). ^{13}C NMR ($CDCl_3$): δ_C, 36.8 (d, J_{PC} 36.8 Hz), 30.6 (d, J_{PC} 39.9 Hz), 30.5 (s), 28.6 (d, J_{PC} 11.5 Hz), 25.3 (d, J_{PC} 2.3 Hz), 24.1 (d, J_{PC} 2.3 Hz), 23.9 (d, J_{PC} 14.6 Hz), 13.8 (s). ^{1}H NMR ($CDCl_3$): δ_H, 2.41-2.34 (2H, br m), 2.25-2.13 (6H, br m), 1.94-1.76 (4H, m), 1.73-1.49 (6H, m), 1.44 (2H, m), 0.95 (3H, t, J_{HH} 7.33 Hz). MS (EI): *m*/*z*, 278.1 (M^+)

General preparation of *s*-PhobP(Se)R. Pure *s*-PhobPR was placed in an NMR tube under N_2. KSeCN (1 eq) in MeOH (0.5 cm^3) was added and the NMR tube was shaken a few times. The reaction was generally complete within 10 min. The solvent was then removed under reduced pressure and the solid residues were extracted with chloroform. Filtration and evaporation of the chloroform gave the desired compound as white solids. Yields were quantitative.

PhobP(=Se)^{i}Bu. PhobP^{i}Bu (0.069 g, 0.35 mmol), KSeCN (0.050 g, 0.35 mmol). ^{31}P NMR (MeOH): δ_P, *s* 35.3 (s, J_{PSe} 674 Hz); a_5 58.4 (s, J_{PSe} 700 Hz); ($CDCl_3$): δ_P, *s* 35.0 (s, J_{PSe} 679 Hz); a_5 58.3 (s, J_{PSe} 703 Hz). HRMS (EI): calcd. for $C_{12}H_{23}PSe$: 278.0703, found 278.0707.

PhobP(=Se)^{s}Bu. PhobP^{s}Bu (0.037 g, 0.19 mmol), KSeCN (0.027 g, 0.19 mmol). ^{31}P NMR (MeOH): δ_P, *s* 48.4 (s, J_{PSe} 679 Hz); a_5 74.2 (s, J_{PSe} 703 Hz); ($CDCl_3$): δ_P, *s* 47.4 (s, J_{PSe} 688 Hz); a_5 73.4 (s, J_{PSe} 712 Hz). HRMS (EI): calcd. for $C_{12}H_{23}PSe$: 278.0703, found, 278.0714.

PhobP(=Se)^{t}Bu. PhobP^{t}Bu (0.039 g, 0.20 mmol), KSeCN (0.028 g, 0.20 mmol). ^{31}P NMR (MeOH): δ_P, *s* 56.2 (s, J_{PSe} 668 Hz); a_7 81.8 (s, J_{PSe} 621 Hz); a_5 87.4 (s, J_{PSe} 698 Hz); ($CDCl_3$): δ_P, *s* 55.1 (s, J_{PSe} 678 Hz); a_7 80.5 (s, J_{PSe} 648 Hz); a_5 86.5 (s, J_{PSe} 705 Hz). HRMS (EI) calcd. for $C_{12}H_{23}PSe$: 278.0703, found, 278.0709.

General preparation of *trans*-[$PtCl_2$(PhobPR)$_2$] A solution of PhobPR (0.25 mmol) in CH_2Cl_2 (1.5 cm^3) was added to a solution of [$PtCl_2$(NC^tBu)$_2$] (50 mg, 0.12 mmol) in CH_2Cl_2 (1.5 cm^3). The mixture was stirred for 2 h, after which the solvent was removed under reduced pressure. The product was recrystallized from pentane to give pale yellow precipitates which were filtered off and dried under reduced pressure. Crystals were obtained by slow evaporation of CH_2Cl_2 solutions of the complexes.

***trans*-[$PtCl_2$(*s*-PhobP^{n}Bu)$_2$] (1a).** Yield: 0.078 g (0.12 mmol, 98%). ^{31}P{^{1}H} NMR (CD_2Cl_2): δ_P 4.1 (s, J_{PPt} 2437 Hz). ^{13}C{^{1}H} NMR (CD_2Cl_2): δ_C 29.5 (s), 26.4 (s), 25.9 (s), 24.4 (t, J_{PC} 12.3 Hz), 22.4 (t, J_{PC} 6.1 Hz), 21.4 (t, J_{PC} 3.8 Hz), 21.4 (s), 20.8 (t, J_{PC} 30.0 Hz), 13.6 (s). ^{1}H NMR (CD_2Cl_2): δ_H 2.69-2.55 (4H, br m), 2.49 (2H, br m), 2.12-1.75 (24H, m), 1.69-1.48 (8H, m), 1.00-0.93 (6H,t). Anal. Calcd for $C_{24}H_{46}Cl_2P_2Pt$: C, 43.51; H, 7.00. Found C, 43.68; H, 7.06. MS (ESI): *m/z* 685.20 $(M+Na)^+$, 626.25 $(M-Cl)^+$, 590.27 $(M-2Cl)^+$.

***trans*-[$PtCl_2$(*s*-PhobP^{i}Bu)$_2$] (1b).** Yield: 0.060 g (0.09 mmol, 82%). ^{31}P NMR (CD_2Cl_2): δ_P, 4.2 (J_{PPt} 2502 Hz), 3.1 (J_{PPt} 2502 Hz). ^{13}C NMR (CD_2Cl_2): δ_C, 30.2 (br s), 30.0 (br s), 27.0 (s), 25.1 (br s), 24.9 (br s), 22.8 (s), 22.3 (br m), 21.9 (s). ^{1}H NMR (CD_2Cl_2): δ_H, 2.61 (4H, br s), 2.43 (4H, br s), 2.12-1.49 (26H, m), 1.16 (6H, d), 1.05 (6H, d). MS (ESI): *m/z* = 590.26 (M^+-2Cl).

***trans*-[PtCl$_2$(*s*-PhobP-(*R*)-^{s}Bu)$_2$] (1c).** Yield: 0.066 g (0.10 mmol, 90%). ^{31}P NMR (CD_2Cl_2): δ_P, 9.3 (J_{PPt} 2493 Hz); 7.7 (J_{PPt} 2614 Hz); the cis isomer (16%) was also detected in the spectrum: 6.2 (J_{PPt} 3352 Hz). Compound insufficiently soluble for ^{13}C NMR. ^{1}H NMR (CD_2Cl_2): δ_H, 2.67-2.47 (br m), 2.36 (br s), 2.26-1.64 (m), 1.22-1.08 (br m). MS (ESI): *m/z* = 590.26 (M^+-2Cl).

***trans*-[PtCl$_2$(*s*-PhobP^{t}Bu)$_2$] (1d).** Yield: 0.070 g (0.12 mmol, 93%). ^{31}P NMR (CD_2Cl_2): δ_P, 19.8 (J_{PPt} 2231 Hz, major), 19.6 (J_{PPt} 2231 Hz, minor). Ratio of isomers, 1.4:1. Compound insufficiently soluble for ^{13}C NMR. ^{1}H NMR (CD_2Cl_2): δ_H, 2.88 (2H, br s), 2.76 (2H, br s), 2.57-1.93 (20H, m), 1.84 (4H, m) 1.53 (18H, t, J_{HH} 7.7 Hz). MS (ESI): *m/z*, 590.26 $(M-2Cl)^+$.

***trans*-[PtCl$_2$(*a*$_5$-PhobP^{n}Bu)$_2$] (2a)**. Yield: 0.073 g (0.11 mmol, 92%). ^{31}P{^{1}H} NMR (CD_2Cl_2): δ_P 40.7 (s, J_{PPt} 2411 Hz). ^{13}C{^{1}H} NMR (CD_2Cl_2): δ_C 32.3 (t, J_{PC} 30.4 Hz), 31.3 (s), 30.1 (t, J_{PC} 7.0 Hz), 26.4 (s), 24.7 (t, J_{PC} 4.7 Hz), 23.5 (t, J_{PC} 12.5 Hz), 23.4 (s), 12.8 (s). ^{1}H NMR (CD_2Cl_2): δ_H 2.66-2.61 (4H, br m), 2.33-2.24 (4H, br m), 2.20-2.09 (8H, m), 1.81-1.1.54 (12H, m), 1.51-1.34 (12H, m), 0.86 (6H, t). Anal. Calcd for $C_{24}H_{46}Cl_2P_2Pt$: C, 43.51; H, 7.00. Found 43.55; H, 6.84. MS (ESI): *m/z* 685.21 $(M+Na)^+$, 590.27 $(M-2Cl)^+$.

***trans*-[PtCl$_2$(*a*$_5$-PhobP^{i}Bu)$_2$] (2b).** Yield: 0.074 g (0.112 mmol, 89 %). ^{31}P{^{1}H} NMR (298 K, 121 MHz, CD_2Cl_2): δ_P 38.4 (s, J_{PPt} 2407 Hz), 37.8 (s, J_{PPt} 2404 Hz). ^{31}P{^{1}H} NMR (373 K, 121 MHz. $C_2H_2Cl_4$): δ_P 38.6 (s, J_{PPt} 2432 Hz). ^{13}C{^{1}H} NMR (400 MHz, CD_2Cl_2): δ_C 34.4 (t, J_{PC} 15.0 Hz), 33.8 (s), 32.2 (s), 31.0 (s), 27.6 (s), 26.3 (s), 25.5 (s), 24.5 (s). ^{1}H NMR (400 MHz, CD_2Cl_2): δ_H 2.70 (4H, br s), 2.58-2.46 (2H, m), 2.44-2.31 (12H, br m), 2.30-2.09 (4H, br m), 1.79-1.66 (4H, br m), 1.64-1.45 (8H, br m), 1.13 (6H, d), 1.10 (6H, d). Anal. Calcd for $C_{24}H_{46}Cl_2P_2Pt$: C, 42.56; H, 7.00. Found C, 43.51; H, 6.56. MS (ESI): *m/z* 590.27 $(M-2Cl)^+$.

***trans*-[PtCl$_2$(*a*$_7$-PhobP^{n}Bu)$_2$] (3a)**. Yield: 0.067 g (0.10 mmol, 85%). ^{31}P{^{1}H} NMR (CD_2Cl_2): δ_P 34.5 (s, J_{PPt} 2311 Hz). ^{13}C{^{1}H} NMR (CD_2Cl_2): δ_C 36.5 (s), 31.0 (t, J_{PC} 29.9 Hz), 29.4 (t, J_{PC} 7.7

Hz), 28.5 (s), 25.2 (s), 24.0 (t, J_{PC} 6.9 Hz), 19.7 (t, J_{PC} 22.3 Hz), 13.7 (s). ^{1}H NMR (CD_2Cl_2): δ_H 3.13 (2H, s), 2.82-1.24 (38H, br m), 0.92 (6H, t). Anal. Calcd for $C_{24}H_{46}Cl_2P_2Pt$: C, 43.51; H, 7.00. Found C, 43.44;H, 7.25. MS (ESI): *m/z* 685.21 $(M+Na)^+$, 626.25 $(M-Cl)^+$, 590.27 $(M-2Cl)^+$.

***trans*-[PtCl$_2$(*a*$_7$-PhobP^{i}Bu)$_2$] (3b).** Yield: 0.078 g (0.117 mmol, 93 %). ^{31}P{^{1}H} NMR (298, 121 MHz, CD_2Cl_2): δ_P 31.6 (s, J_{PPt} 2505 Hz). ^{31}P{^{1}H} NMR (173 K, 121 MHz, CH_2Cl_2): δ_P 33.7 (s, J_{PPt} 2261 Hz), 32.9 (s, J_{PPt} 2255 Hz). ^{13}C{^{1}H} NMR (400 MHz, CD_2Cl_2): δ_C 31.9 (s), 31.7 (s), 31.6 (s), 29.4 (t, J_{PC} 7.50 Hz), 29.0 (s), 27.4 (s), 25.2 (s), 23.8 (s). ^{1}H NMR (400 MHz, CD_2Cl_2): δ_H 3.11 (4H, s), 2.61-2.43 (2H, br m), 2.42-2.31 (5H, br m), 2.01-1.92 (5H, m), 1.92-1.72 (8H, br m), 1.71-1.43 (10H, br m), 1.10 (6H, d), 1.08 (6H, d). Anal. Calcd for $C_{24}H_{46}Cl_2P_2Pt$: C, 43.51; H. 7.00. Found 42.52; H, 6.78. MS (ESI): *m/z* 590.27 $(M-2Cl)^+$.

General preparation of *trans*-[PdCl$_2$(PhobPR)$_2$] A solution of a pure *s-, a*$_5$- or *a*$_7$-isomer of PhobPR (0.050 g, 0.25 mmol) in CH_2Cl_2 (2.0 cm^3) was added to a solution of $[PdCl_2(NCPh)_2]$ (0.048 g, 0.13 mmol) in CH_2Cl_2 (2.0 cm^3). The mixture was stirred for 2 h after which the solvent was removed under reduced pressure. The products were recrystallized from pentane to give white precipitates which were filtered off and dried under reduced pressure.

***trans*-[PdCl$_2$(*s*-PhobP^{n}Bu)$_2$] (4a).** Yield: 0.0416 g (0.073 mmol, 58%). ^{31}P{^{1}H} NMR (298 K, 121 MHz, CD_2Cl_2): δ_P 9.52 (s). ^{31}P{^{1}H} NMR (173 K, 121 MHz, CH_2Cl_2): δ_P 10.2 (s), 9.33 (s). ^{13}C{^{1}H} NMR (500 MHz, CD_2Cl_2): δ_C 30.6 (s), 29.8 (s), 26.8 (t, J_{PC} 1.91 Hz), 24.5 (s), 24.4 (s), 22.52 (s), 22.4 (s), 22.3 (t, J_{PC} 3.82 Hz), 21.4 (s), 21.2 (s), 18.0 (s), 13.6 (s). ^{1}H NMR (500 MHz, CD_2Cl_2): δ_H 2.59-2.51 (8H, br m), 2.15 (8H, s), 2.11-1.84 (18H, br m), 1.55 (6H, s), 0.99 (6H, t). Anal Calcd for $C_{26}H_{46}Cl_2P_2Pd$:C, 50.23; H, 8.08. Found C, 50.51; H, 8.03. MS (ESI): *m/z* 537.18 $(M-Cl)^+$, 501.21 (M-2Cl).

***trans*-[PdCl$_2$(*s*-PhobP^{i}Bu)$_2$] (4b).** Yield: 0.0293 g (0.051 mmol, 41%). ^{31}P{^{1}H} NMR (298 K, 121 MHz, CD_2Cl_2): δ_P 9.01 (s), 7.73 (s). ^{31}P{^{1}H} NMR (373 K, 121 MHz, $C_2H_2Cl_4$): δ_P 7.68 (s).

$^{13}C\{^1H\}$ NMR (500 MHz, CD_2Cl_2): δ_C 30.5 (br s), 29.9 (br s), 26.9 (s), 24.6 (br s), 23.4 (br s), 22.1 (s), 21.2 (s), 20.3 (s). ^1H NMR (400 MHz, CD_2Cl_2): δ_H 2.65-2.50 (10H, br m), 2.13-1.82 (20H, br m), 1.66 (3H, t), 1.54 (1H, s), 1.22 (6H, d), 1.18 (6H, d). Anal Calcd for $C_{26}H_{46}Cl_2P_2Pd$: C, 50.23; H, 8.08. Found C, 50.61; H, 7.96. MS (ESI): *m/z* 501.20 (M-2Cl).

***trans*-[PdCl$_2$(*a*$_5$-PhobP^{n}Bu)$_2$] (5a).** Yield: 0.0316 g (0.055 mmol, 44%). $^{31}P\{^1H\}$ NMR (298 K, 121 MHz, CD_2Cl_2): δ_P 48.1. $^{31}P\{^1H\}$ NMR (193 K, 121 MHz, CH_2Cl_2): δ_P 48.2 (s), 48.0 (s). $^{13}C\{^1H\}$ NMR (500 MHz, CD_2Cl_2): δ_C 34.3 (t, J_{PC} 12.4 Hz), 32.4 (s), 30.6 (t, J_{PC} 2.86 Hz), 27.8 (br s), 25.8 (t, J_{PC} 1.91 Hz), 24.50 (s), 24.45 (s), 24.40 (s), 24.1 (t, J_{PC} 9.54 Hz), 13.5 (s). ^1H NMR (500 MHz, CD_2Cl_2): δ_H 2.72 (4H, br s), 2.41 (4H, br s), 2.27-2.15 (8H, br m), 1.89-1.49 (18H, br m), 0.98 (6H, t). Anal. Calcd for $C_{26}H_{46}Cl_2P_2Pd$: C, 50.23; H, 8.08. Found C, 51.03; H, 8.26. MS (ESI): *m/z* 501.21 (M-2Cl).

***trans*-[PdCl$_2$(*a*$_5$-PhobP^{i}Bu)$_2$] (5b).** Yield: 0.0393 g (0.068 mmol, 54%). $^{31}P\{^1H\}$ NMR (298 K, 121 MHz, CD_2Cl_2): δ_P 46.5 (s), 45.9 (s). $^{31}P\{^1H\}$ NMR (373 K, 121 MHz, $C_2H_2Cl_4$): δ_P 46.4 (s). $^{13}C\{^1H\}$ NMR (500 MHz, CD_2Cl_2): δ_C 35.6 (t, J_{PC} 12.4 Hz), 32.5 (s), 30.7 (t, J_{PC} 2.86 Hz), 25.7 (br s), 24.6 (t, J_{PC} 3.81 Hz). ^1H NMR (400 MHz, CD_2Cl_2): δ_H 2.73 (4H, s), 2.60-2.35 (6H, br m), 2.27-2.13 (8H, br m), 1.71 (4H, q), 1.62-1.40 (12H, br m), 1.18 (6H, d), 1.16 (6H, d). Anal. Calcd for $C_{26}H_{46}Cl_2P_2Pd$: C, 50.23; H 8.08. Found 50.86; H, 8.29. MS (ESI): *m/z* 536.18 (M-Cl), 501.20 (M-2Cl).

***trans*-[PdCl$_2$(*a*$_7$-PhobP^{n}Bu)$_2$] (6a).** Yield: 0.0248 g (0.051 mmol, 34%). $^{31}P\{^1H\}$ NMR (298 K, 121 MHz, CD_2Cl_2): δ_P 39.5. $^{31}P\{^1H\}$ NMR (173 K, 121 MHz, CH_2Cl_2): δ_P 40.1 (s), 39.7 (s). $^{13}C\{^1H\}$ NMR (500 MHz, CD_2Cl_2): δ_C 32.4 (t, J_{PC} 12.4 Hz), 31.5 (t, J_{PC} 1.91 Hz), 29.5 (t, J_{PC} 8.58 Hz), 29.0 (t, J_{PC} 2.86 Hz), 25.2 (s), 24.1 (t, J_{PC} 5.72 Hz), 20.0 (t, J_{PC} 7.63 Hz), 13.6 (s). ^1H NMR (500 MHz, CD_2Cl_2): δ_H 3.15 (4H, br s), 2.36 (4H, br s), 2.14 (2H, s), 1.91-1.51 (18H, br s),

0.98 (6H, t). Anal. Calcd for $C_{26}H_{46}Cl_2P_2Pd$: C, 50.23; H, 8.08. Found C, 50.22; H, 8.15. MS (ESI): *m/z* 501.21 (M-2Cl).

***trans*-[PdCl$_2$(*a*$_7$-PhobP^{i}Bu)$_2$] (6b).** Yield: 0.0345 g (0.060 mmol, 48%). $^{31}P\{^1H\}$ NMR (298 K, 121 MHz, CD_2Cl_2): δ_P 38.6 (s). $^{31}P\{^1H\}$ NMR (173 K, 121 MHz, CH_2Cl_2): δ_P 38.5 (s), 38.1 (s). $^{13}C\{^1H\}$ NMR (500 MHz, CD_2Cl_2): δ_C 33.0 (t, J_{PC} 12.4 Hz), 31.7 (s), 30.6 (s), 29.5 (s), 29.5 (t, J_{PC} 2.86 Hz), 29.4 (s), 27.7 (t, J_{PC} 1.91 Hz), 25.1 (s), 23.9 (t, J_{PC} 4.77 Hz). ^1H NMR (400 MHz, CD_2Cl_2): δ_H 3.12 (4H, br s), 2.49-2.37 (6H, br m), 2.13 (8H, s), 1.96-1.63 (22 H, br m), 1.15 (6H, t). Anal. Calcd for $C_{26}H_{46}Cl_2P_2Pd$: C, 50.23; H, 8.08. Found 50.42; H, 8.23. MS (ESI): *m/z* 536.18 (M-Cl), 501.20 (M-2Cl).

Crystal structure determinations. X-ray diffraction experiments on all crystals were carried out at 100 K on a Bruker APEX II diffractometer using Mo-K_α radiation (λ = 0.71073 Å). Data collections were performed using a CCD area detector from a single crystal mounted on a glass fibre. Intensities were integrated[24] from several series of exposures measuring 0.5° in ω or ϕ. Absorption corrections were based on equivalent reflections using SADABS.[25] The structures were solved using SHELXS and refined against all F_o^2 data with hydrogen atoms riding in calculated positions using SHELXL.[26] Crystal structure and refinement data are given in Table 3. Minor disorder of the phobane ring was modeled for **2a** (36%), **3b** (22%), **5b** (50%) and **6b** (25%), whilst **5b** had dynamic disorder of one its ^{i}Bu substituent (16%). Data for crystal **2b** were twinned. The different components of the non-merohedral twins were assigned using the Bruker program CELL_NOW[27] and corrected for absorption with TWINABS[28]. The difference map shows large features (*ca*. 4 eÅ^{-3}) close to (≤ 1 Å) the platinum and palladium atoms, presumably due to absorption effects, but no features of chemical significance. Collection of data for crystal **2a** was not completed to normal levels of completeness due to instrument failure.

Computational Details. DFT calculations were computed in the gas-phase with the Jaguar program,[29] using the standard hybridized functional B3LYP[30] and basis-set combination 6-31G for all atoms, with the exception of Pd and Pt atoms for which the effective core potential LACV3P basis set was used instead. Rotations were carried out in increments of 30° by constraining the Cl-metal-P-$C1_R$ torsion.

Acknowledgements. Thanks to Shell and EPSRC for studentships. The Royal Society, COST action CM0802 "PhoSciNet" and the CCDC for supporting this work and Johnson-Matthey for a loan of precious metal compounds.

Supporting Information Available. Details of the computational work, cif files and/or text files reporting crystal and refinement data are provided for all crystal structures. This material is available free of charge via the Internet at http://pubs.acs.org.

Table 3 Crystal data.

Compound	*s*-PhobP(Se)^{n}Bu	a_7-PhobP(Se)^{n}Bu	a_5-PhobP(Se)^{n}Bu
Color, habit	colorless block	colorless block	colorless block
Size/mm	0.67×0.16×0.14	0.24×0.18×0.18	0.35×0.26×0.22
Empirical Formula	$C_{12}H_{23}PSe$	$C_{12}H_{23}PSe$	$C_{12}H_{23}PSe$
M	277.23	277.23	277.23
Crystal system	triclinic	triclinic	monoclinic
Space group	*P*-1	*P*-1	$P2_1/n$
a/Å	7.0652(10)	7.3002(2)	11.9319(4)
b/Å	9.8344(14)	9.1583(2)	8.9612(3)
c/Å	10.6283(16)	10.1355(2)	13.2301(5)
α/°	115.834(6)	111.174(1)	90.00
β/°	101.468(5)	93.095(1)	113.1560(10)
γ/°	92.320(6)	92.187(1)	90.00
V/Å^3	644.60(16)	629.75(3)	1300.65(8)
Z	2	2	4
μ/mm^{-1}	3.001	3.072	2.975
T/K	120	100	100
$\theta_{min,max}$	3.65,36.21	2.57,27.63	1.95,27.53
Completeness	0.975 to θ = 27.50°	0.990 to θ = 27.63°	0.998 to θ = 27.53°
Reflections: total/independent	18717/4408	18811/2897	15293/2992
R_{int}	0.0291	0.0209	0.0221
Final *R*1 and *wR*2	0.0151, 0.0402	0.0228, 0.0610	0.0191, 0.0503
Largest peak, hole/eÅ^{-3}	0.380, -0.299	0.596, -0.378	0.640, -0.270
ρ_{calc}/g cm^{-3}	1.428	1.462	1.416

Compound	**2a**	**4a**
Color, habit	colorless block	yellow block
Size/mm	0.14×0.06×0.06	0.25×0.24×0.22
Empirical Formula	$C_{24}H_{46}Cl_2P_2Pt$	$C_{24}H_{46}Cl_2P_2Pd$
M	662.54	573.85
Crystal system	monoclinic	triclinic
Space group	$P2_1/n$	P-1
a/Å	8.1637(6)	7.7650(3)
b/Å	7.8841(6)	7.8175(4)
c/Å	20.4032(17)	11.0564(5)
α/°	90.00	97.289(3)
β/°	98.787(6)	103.064(3)
γ/°	90.00	96.625(3)
V/Å^3	1311.67(18)	641.25(5)
Z	2	1
μ/mm^{-1}	5.684	1.067
T/K	100	100
$\theta_{min,max}$	2.74,28.48	1.91,27.48
Completeness	0.896 to θ = 28.48°	0.988 to θ = 27.48°
Reflections: total/independent	23807/4981	6756/2914
R_{int}	0.0652	0.0252
Final $R1$ and $wR2$	0.0585,0.1090	0.0556,0.1441
Largest peak, hole/eÅ^{-3}	3.261,-1.975	3.501,-1.223
ρ_{calc}/g cm^{-3}	1.678	1.496

Compound	**1b**	**2b**	**3b**
Color, habit	colorless plate	yellow prism	yellow block
Size/mm	0.55×0.46×0.32	0.20×0.28×0.37	0.25×0.134×0.11
Empirical Formula	$C_{24}H_{46}Cl_2P_2Pt$	$C_{24}H_{46}Cl_2P_2Pt$	$C_{24}H_{46}Cl_2P_2Pt$
M	662.54	662.54	662.54
Crystal system	triclinic	monoclinic	monoclinic
Space group	*P*-1	$P2_1/n$	$P2_1/c$
a/Å	8.3578(3)	11.9830(10)	10.0716(13)
b/Å	9.1768(3)	12.2971(10)	17.273(2)
c/Å	9.3694(3)	18.1806(16)	15.466()2)
α/°	85.464(2)	90.00	90.00
β/°	65.173(2)	101.331(5)	93.564(7)
γ/°	86.866(2)	90.00	90.00
V/Å^3	649.97(4)	2626.8(4)	2685.3(6)
Z	1	4	4
μ/mm^{-1}	5.736	5.677	5.553
T/K	100	100	100
$\theta_{min,max}$	2.23,27.50	2.40,21.42	1.77,27.56
Completeness	0.998 to θ = 27.50°	0.971 to θ = 32.35°	0.995 to θ = 27.56°
Reflections: total/independent	10950/2984	9243/9243	89368/6172
R_{int}	0.0207	-	0.0295
Final *R*1 and *wR*2	0.0180,0.0456	0.0645,0.1073	0.0189,0.0441
Largest peak, hole/eÅ^{-3}	1.644,-0.967	4.432,-2.283	2.080,-1.384
ρ_{calc}/g cm^{-3}	1.693	1.675	1.639

Compound	**4b**	**5b**	**6b**
Color, habit	yellow plate	yellow plate	colorless plate
Size/mm	0.46×0.34×0.21	0.55×0.41×0.34	××
Empirical Formula	$C_{24}H_{46}Cl_2P_2Pd$	$C_{24}H_{46}Cl_2P_2Pd$	$C_{24}H_{46}Cl_2P_2Pd$
M	573.85	573.85	573.85
Crystal system	triclinic	monoclinic	monoclinic
Space group	*P*-1	*C*2/*c*	$P2_1/c$
a/Å	8.3609(7)	19.5252(5)	10.0704(3)
b/Å	9.1728(9)	16.2838(4)	17.3101(4)
c/Å	9.3913(9)	8.8634(2)	15.4017(4)
α/°	85.750(5)	90.00	90.00
β/°	64.862(5)	109.9410(10)	93.5110(10)
γ/°	86.813(5)	90.00	90.00
V/Å^3	650.00(10)	2649.11(11)	2679.78(12)
Z	1	4	4
μ/mm^{-1}	1.052	1.033	1.021
T/K	100	100	100
$\theta_{min,max}$	2.40,25.74	2.22,26.47	2.65,42.32
Completeness	0.982 to θ = 25.74°	0.998 to θ = 27.52°	0.978 to θ = 42.48°
Reflections: total/independent	14405/2442	28470/3062	72832/18812
R_{int}	0.0902	0.0388	0.0299
Final *R*1 and *wR*2	0.0692,0.1808	0.0296,0.720	0.0433,0.0933
Largest peak, hole/eÅ^{-3}	3.178,-1.386	0.672,-0.352	3.499,-2.663
ρ_{calc}/g cm^{-3}	1.466	1.439	1.422

(1) Carreira, M.; Charernsuk, M.; Eberhard, M.; Fey, N.; van Ginkel, R.; Hamilton, A.; Mul, W. P.; Orpen, A. G.; Phetmung, H.; Pringle, P. G. *J. Am. Chem. Soc.* **2009**, *131*, 3078 and references therein.

(2) (a) Mulders, J. P. *Neth. Patent* **1966**, 6 604 09 to Shell. (b) Winkle, J. L. V.; Mason, R. F. *U. S. Patent* **1968**, 3 400 163 to Shell.

(3) (a) Drent, E.; Van Broekhoven, J. A. M.; Breed, A. J. M. *World Patent* **2003**, WO 03040065 to Shell. (b) Eberhard, M. R.; Carrington-Smith, E.; Drent, E. E.; Marsh, P. S.; Orpen, A. G.; Phetmung, H.; Pringle, P. G. *Adv. Synth. Catal.* **2005**, *347*, 1345. (c) Konya, D.; Lenero, K. Q. A.; Drent, E. *Organometallics* **2006**, *25*, 3166. (d) Dwyer, C. L.; Kirk, M. M.; Meyer, W. H.; van Rensburg, W. J.; Forman, G. S. *Organometallics* **2006**, *25*, 3806. (e) Boeda, F.; Clavier, H.; Jordaan, M.; Meyer, W. H.; Nolan, S. P. *J. Org. Chem.* **2008**, *73*, 259. (f) Lewis, J. C.; Berman, A. M.; Bergman, R. G.; Ellman, J. A. *J. Am. Chem. Soc.* **2008**, *130*, 2493. (g) Butti, P.; Rochat, R.; Sadow, A.D; Togni, A. *Angew. Chem. Int. Ed,* **2008**, *47,* 4878. (h) Wolf, J.; Thommes, K.; Briel, O.; Scopelliti, R.; Severin, K. *Organometallics* **2008**, *27*, 4464. (i) Hansen, K. B.; Hsiao, Y.; Xu, F.; Rivera, N.; Clausen, A.; Kubryk, M.; Krska, S.; Rosner, T.; Simmons, B.; Balsells, J.; Ikemoto, N.; Sun, Y.; Spindler, F.; Malan, C.; Grabowski, E. J. J.; Armstrong, J. D. *J. Am. Chem. Soc.* **2009**, *131*, 8798. (j) Marx, F. T. I.; Johan H. L. Jordaan, J. H. L.; Vosloo, H. C. M. *J. Mol. Model.* **2009**, *15*, 1371. (k) Sauvage, X.; Zaragoza, G.; Demonceau, A. Delaude, L. *Adv. Synth. Catal.* **2010**, *352*, 1934. (l) Miao, X.; Malacea, R.; Fischmeister, C.; Bruneau, C.; Dixneuf, P. H. *Green Chem.* **2011**, *13*, 2911. (m) Scholz, J.; Loekman, S.; Szesni, N.; Hieringer, W.; Goerling, A.; Haumann, M.; Wasserscheid, P. *Adv. Synth. Catal.* **2011**, *353*, 2701. (n) Miao, X.; Malacea, R.; Fischmeister, C.; Bruneau, C.; Dixneuf, P. H. *Green Chem.* **2011**, *13*, 2911. (o)

Scholz, J.; Loekman, S.; Szesni, N.; Hieringer, W.; Goerling, A.; Haumann, M.; Wasserscheid, P. *Adv. Synth. Catal.* **2011**, *353*, 2701. (p) Behr, A.; Krema and A. Kämper *RSC Advances* **2012**, *2*, 12775. (q) Ohlmann, D. M.; Tschauder, N.; Stockis, J-P.; Goossen, K.; Dierker, M.; Goossen, L. J. *J. Am. Chem. Soc.* **2012**, *134*, 13716. (r) Montenegro, R. E.; Meier, M. A. R. *Eur. J. Lipid Sci. Tech.* **2012**, *114*, 55. (s) Birbeck, J. M.; Haynes, A.; Adams, H.; Damoense, L.; Otto S. *ACS Catal.* **2012**, *2*, 2512. (t) von Czapiewski, M.; Kreye, O.; Mutlu, H.; Meier, M. A. R. *Eur. J. Lipid Sci. Tech.* **2013**, *115*, 76. (u) Raoufmoghaddam, S.; Drent, E.; Bouwman, E. *Adv. Synth. Catal.* **2013**, *355*, 717.

(4) (a) Smith, A. E. *Inorg. Chem.* **1972**, *11*, 3017. (b) Abbenhuis, H. C. L.; Burckhardt, U.; Gramlich, V.; Koelner, C.; Pregosin, P. S.; Salzmann, R.; Togni, A. *Organometallics* **1995**, *14*, 759. (c) Coles, S. J.; Edwards, P. G.; Hursthouse, M. B.; Abdul Malik, K. M.; Thick, J. L.; Tooze, R. P. *J. Chem. Soc. Dalton Trans.* **1997**, 1821. (d) Dunne, J. P.; Aiken, S.; Duckett, S. B.; Konya, D.; Leñero, K. Q. A.; Drent, E. *J. Am. Chem. Soc.* **2004**, *126*, 16708. (e) Eberhard, M. R.; Heslop, K. M.; Orpen, A. G.; Pringle, P. G. *Organometallics* **2005**, *24*, 335. (f) Bungu, P. N.; Otto, S. *Dalton Trans.* **2007**, 2876. (g) Bungu, P. N.; Otto, S. *J. Organomet. Chem.* **2007**, *692*, 3370. (h) Lopez-Serrano, J.; Duckett, S. B.; Aiken, S.; Leñero, K. Q. A.; Drent, E.; Dunne, J. P.; Konya, D.; Whitwood, A. C. *J. Am. Chem. Soc.* **2007**, *129*, 6513. (i) Baya, M.; Houghton, J.; Konya, D.; Champouret, Y.; Daran, J.-C.; Almeda Leñero, K. Q.; Schoon, L.; Mul, W. P.; van Oort, A. B.; Meijboom, N.; Drent, E.; Orpen, A. G.; Poli, R. *J. Am. Chem. Soc.* **2008**, *130*, 10612. (j) Bungu, P. N.; Otto, S. *Dalton Trans.* **2011**, *40*, 9238. (k) Fey, N.; Garland, M; Hopewell, J. P.; McMullin, C. L.; Mastroianni, S.; Orpen, A. G.; Pringle, P. G. *Angew. Chem., Int. Ed.* **2012**, *51*, 118.

(5) (a) Mann, B. E., Masters, C.; Shaw, B. L.; Stainbank, R. E. *Chem. Commun*. **1971**, 1103. (b) Bright, A.; Mann, B. E., Masters, C.; Shaw, B. L.; Slade, R. M.; Stainbank, R. E. *J. Chem. Soc. (A)* **1971**, 1826. (c) Empsall, H. D.; Hyde, E. M.; Mentzer, E.; Shaw, B. L. Baber, R. A. *J. Chem. Soc. Dalton Trans*. **1977**, 2285. (d) Shaw, B. L. *J. Organometallic Chem*. **1980**, *200*, 307.

(6) (a) Bushweller, C. H.; Hoogasian, S.; English, A. D.; Miller, J. S.; Lourandos, M. Z. *Inorg. Chem*. **1981**, *20*, 3448. (b) Topping, R. J.; Quin, L. D.; Crumbliss, A. L. *J. Organomet. Chem*. **1990**, *385*, 131. (c) Asaro, F.; Garlatti, R. D.; Pellizer, G.; Tauzher, G. *Inorg. Chim. Acta* **1993**, *211*, 27. (d) Albert, J.; Bosque, R.; Cadena, J. M.; Delgado, S.; Granell, J. *J. Organomet. Chem*. **2001**, *634*, 83. (e) Orpen, A. G.; Pringle, P. G.; Wilkinson, M. J.; Wingad, R. L. *Dalton Trans*. **2005**, 659. (f) Jankowski P.; McMullin C. L.; Gridnev I. D.; Orpen A. G.; Pringle P. G. *Tetrahedron Asym*. **2010**, *21,* 1206. (g) Kinzel T.; Zhang Y.; Buchwald S. L. *J. Am. Chem. Soc*., **2010**, *132*, 14073. (h) Alberico E.; Baumann W.; de Vries, J G.; Drexler H.-J.; Gladiali, S.; Heller, D.; Henderickx, H. J. W.; Lefort, L. *Chem. Eur. J*. **2011**, *17*, 12683..

(7) Doherty, S.; Knight J. G.; Ward N. A. B.; Bittner, D. M.; Wills C.; McFarlane W.; Clegg W.; Harrington R. W. *Organometallics* **2013**, *32*, 1773 and references therein.

(8) Robertson, A. P. *World Patent* **2000**, WO 00/52017 to Cytec.

(9) Muller, A.; Otto, S.; Roodt, A. *Dalton Trans*. **2008**, 650 and refs therein.

(10) Hitchcock P. B.; Jacobson B.; Pidcock A. *J. Chem. Soc. Dalton Trans*. **1977**, 2038.

(11) (a) Redfield, D. A.; Nelson, J. H.; Cary, L.W. *Inorg. Nucl. Chem. Lett*. **1974**, *10*, 727. (b) Pregosin P. S.; Kunz, R. *Helv. Chim. Acta* **1975**, *58*, 423. (c) van den Beuken, E.K.; Meetsma,

A.; Kooijman, H.; Spek A. L.; Feringa, B.L. *Inorg. Chim. Acta* **1997**, *264*, 171. (d) Andreasen, L. V.; Simonsen O.; Wernberg, O. *Inorg. Chim. Acta* **1999**, *295*, 153.

(12) Friebolin H. in *Basic One- and Two-Dimensional NMR Spectroscopy*, Wiley 2010.

(13) (a) McMullin, C. L.; Jover, J.; Fey, N.; Harvey, J. N. *Dalton Trans.* **2010**, *39*, 10833. (b) Fey, N.; Ridgway, B. M.; Jover, J.; McMullin, C. L.; Harvey, J. N. *Dalton Trans.* **2011**, *40*, 9042.

(14) Pitter, S.; Dinjus, E.; Jung, B.; Gorls, H. *Z. Naturforsch., B.* **1996**, *51*, 934. CSD REF = HIJJEP

(15) Dwyer, C. L.; Kirk, M. M.; Meyer, W. H.; van Rensburg, W. J.; Forman, G. S. *Organometallics* **2006**, *25*, 3806.

(16) (a) Buchwald, S. L.; Mauger C.; Mignani G.; Scholz, U. *Adv. Synth. Catal.* **2006**, *348*, 23. (b) Hartwig, J. F. *Acc. Chem. Res.* **2008**, *41*, 1534. (c) Surry, D. S.; Buchwald, S. L. *Angew. Chem., Int. Ed.* **2008**, *47*, 6338. (c) Hill, L. L.; Crowell, J. L.; Tutwiler, S. L.; Massie, N. L.; Hines, C. C.; Griffin, S. T.; Rogers, R. D.; Shaughnessy, K. H.; Grasa, G. A.; Johansson Seechurn, C. C. C.; Li H.; Colacot, T. J. ; Chou J.; Woltermann C. J. *J. Org. Chem.* **2010**, *75*, 6477. (d) Busacca, C. A.; Fandrick, D. R.; Song, J. J.; Senanayake, C. H. *Adv. Synth. Catal.* **2011**, *353*, 1825. (e) Raders, S. M.; Moore, J. N.; Parks, J. K.; Miller, A. D.; Leissing, T. M.; Kelley, S. P.; Rogers, R. D.; Shaughnessy, K. H. *J. Org. Chem.* **2013**, *78*, 4649.

(17) Fanjul, T.; Eastham, G.; Floure, J.; Forrest, S. J. K.; Haddow, M. F.; Hamilton, A.; Pringle, P. G.; Orpen, A. G.; Waugh, M. *Dalton Trans.*, **2013**, *42*, 100 and references therein.

(18) For recent reviews of PCP pincer complexes, see: (a) Gelman, D; Musa, S. *ACS Catalysis* **2012**, *2*, 2456. (b) Haibach, M. C.; Kundu, S.; Brookhart, M.; Goldman, A. S. *Acc. Chem. Res.*

2012, *45*, 947. (c) Gunanathan, C.; Milstein, D. *Acc. Chem. Res.* **2011**, *44*, 588. (d) Selander, N.; Szabo, K. J. *Chem. Rev.* **2011**, *111*, 2048.

(19) Pangborn, A. B.; Giardello, M. A.; Grubbs, R. H.; Rosen R. K.; Timmers, F. J. *Organometallics* **1996**, *15*, 1518.

(20) Fraccarollo, D.; Bertani, R.; Mozzon, M.; Belluco, U.; Michelin, R. A. *Inorg. Chim. Acta* **1992**, *201*, 15.

(21) Kharasch, M. S.; Seyler, R. C.; Mayo, F. R. *J. Am. Chem. Soc.* **1938**, *60*, 882.

(22) Umemura, K.; Matsuyama, H.; Kamigata, N. *Bull. Chem. Soc. Jpn.* **1990**, *63*, 2593.

(23) Dodds, D. L.; Floure, J.; Garland, M.; Haddow, M. F.; Leonard, T. R.; McMullin, C. L.; Orpen, A. G.; Pringle, P. G. *Dalton Trans.* **2011**, *40*, 7137.

(24) Bruker-AXS SAINT, Madison, Wisconsin.

(25) Sheldrick, G. M. SADABS V2008/1, University of Göttingen, Germany.

(26) Sheldrick, G. M. *Acta Cryst.* **2008**, *A64,* 112.

(27) Sheldrick G. M. **2008**, CELL NOW v2008/2, Bruker AXS Inc., Madison, Wisconsin, USA.

(28) Sheldrick G. M. **2008**, TWINABS v2008/2, Bruker AXS Inc., Madison, Wisconsin, USA.

(29) Schrödinger, L. *Jaguar, 6.0*; Schrödinger , LLC: New York, 2005.

(30) (a) Becke, A. D. J. *Chem. Phys.* **1993**, *98*, 5648. (b) Lee, C., Yang, W., Parr, B. G. *Phys. Rev. B* **1988**, *37*, 785. (c) Vosko, S. H., Wilk, L., Nusair, M. *Can J. Phys.* **1980**, *58*, 1200. (d) Stephens, P. J., Devlin, F. J., Chabalowski, C. F., Frisch, M. J. *J. Phys. Chem.* **1994**, *98*, 11623.